JTBB
Journal of Tropical Biodiversity and Biotechnology
online http://jtbb.or.id
ISSN 2540-9581 (online)

Journal of Tropical Biodiversity and Biotechnology

Volume 4, Issue 3, December 2019

Published by:

Faculty of Biology
Universitas Gadjah Mada

In collaboration with:

KOBI

KONSORSIUM BIOTEKNOLOGI INDONESIA
Indonesian Biotechnology Consortium

J.Trop. Biodiv.Biotech.	Volume 4	Issue 3	Page 90 - 124	Yogyakarta December 2019	ISSN 2540-9581

Table of Contents

Journal of Tropical Biodiversity and Biotechnology
Volume 04, Issue 03 (2019): 90 — 96
DOI: 10.22146/jtbb.38749

Research Article

Empty Fruit Bunches as Potential Source for Biosilica Fertilizer for Oil Palm

Laksmita Prima Santi[1]*, Donny Nugroho Kalbuadi[1], Didiek Hadjar Goenadi[1]
1) Indonesian Research Institute for Biotechnology and Bioindustry, PT Riset Perkebunan Nusantara, Bogor, Indonesia

Corresponding author, email address: laksmita.santi@gmail.com

Keywords:
bio silica
silica body
empty fruit bunch
bio decomposition
mono silicic acid

Article history:
Submitted 13/09/2018
Revised 28/09/2019
Accepted 30/09/2019

ABSTRACT
In Indonesia, the development of oil palm plantations has been going on a pervasive way; they covered about 14.03 million hectares in 2017. This massive coverage of land might then generate a tremendous amount of biomass per year, both in the form of both solid and liquid wastes. The processing of fresh fruit bunches (FFB) in palm oil mill (POM) produces wastes that primarily in the form of empty fruit bunches (EFB), which is amounting of up to 25% (w/w) of FFB. It has been being indicated that EFB contains a considerable amount of silica (Si) which attracts the Indonesian Research Institute for Biotechnology and Bioindustry (IRIBB) to investigate the potential use of EFB as a source of bio-available Si, in the form of H_4SiO_4 (mono silicic acid, BioSilAc). The experiment was carried out at Sungai Mirah Minting Estate, PT Bumitama Gunajaya Agro-Central Kalimantan. The EFB material was obtained from POM and chopped into 2.5-5.0 cm in size. A four-week bio-decomposition process was employed by using bio-decomposers containing *Trichoderma pseudokoningii*, *T. polysporum*, and *Phanerochaete chrysosporium*. Chemical analyses of composted EFB were conducted before and 28-days after decomposer application. The presence of Si in the compost was observed by scanning electron microscopy (SEM). The effect of Si-containing EFB compost on the immature and mature oil palm was evaluated. Seven treatments, i.e. combination of EFB compost and BioSilAc application with reduced-dosages of NPK fertilisers were arranged in a random block design with three replicates. The results show that large quantities of silica bodies attached to the surface of EFB fibres and amounting to 0.44% soluble Si. The FFB data indicated that the application of 75% NPK + 500 kg composted EFB + 2 L BioSilAc/ha/year on a five-year-old plant resulted in higher yield than that obtained from 100% standard dosage of NPK. The study also revealed that the application of EFB compost reduced 50% of BioSilAc dosage.

INTRODUCTION
Indonesia has been placed as the world's first producer of palm kernel and crude palm oils. In producing crude palm oil (CPO) and palm kernel oil (PKO), the oil palm industry is strongly dependent on the processing of the fresh fruit bunches (FFB) at palm oil mill (POM) and traded internationally. However, this process produces also a waste of solid organic waste [i.e. empty fruit bunch (EFB)], which reaches up to 25% of FFB. Therefore, if Indonesia produced 38 million tons of CPO in 2017, then it is equivalent to 190 million tons of FFB. Since FFB yielded in 20% CPO, it leads to the potential availability of EFB more than 47 million tons per year. In addition to the production of solid waste, the POM also produces nonsolid biomass called as palm oil mill effluent (POME) in huge quantity, material discharged from washing and sterilization of the palm fruits.

Oil palm EFB fiber has been identified as the single most important agriculture biomass in Indonesia was usually contains 30–35% lignocellulose, 1–3% residue oil, and roughly 60% of moisture (Gunawan *et al.* 2009). The lignocellulose or fiber consists of cellulose, hemicellulose, and lignin. Many types of research on EFB had been

focused on energy, biochemicals, and wood-related products development purposes (Geng, 2013) as well as for compost (Goenadi, 2006). Therefore, this material could become an important portfolio to sustain the development and growth of energy demand, biochemicals, industrial materials, and sources of available nutrients for the plant. It has also been indicated that EFB contains a considerable amount of silica (Si) so then the Indonesian Research Institute for Biotechnology and Bioindustry (IRIBB) has investigated the potential use of EFB as a source of bio-available Si, in the form of H_4SiO_4 (mono silicic acid) (Santi *et al.* 2017). The IRIBB has also developed a bio-available Si product derived from quartz sand enriched with Si-solubilizing microbes (BioSilAc).

Silica (Si) is the second most abundant element in soils and can be found in noticeable concentrations in many terrestrial plants (Epstein, 1994; Keeping & Reynolds, 2009). Plant species vary in their ability to take up and accumulate Si as silicon dioxide (SiO_2) in their tissues; depends on this characteristic, plants are then classified as excluders, intermediate types, or accumulators (Mitani & Ma, 2005; Montpetit *et al.* 2012). Most dicots accumulate less than 0.1% Si on a dry weight basis, but many grasses species are able to accumulate as much as 10% (Montpetit *et al.* 2012; Ma *et al.* 2002; Vivancos *et al.* 2015). It has been widely reported that Si is able to suppress both physical stresses, such as drought, high temperature, UV, loading, and freezing, and chemical stress, including salinity, nutrient imbalance, and metal toxicity (Ma, 2004; Ma & Yamaji 2015). Silica has not been recognized as an essential element, although numerous studies have demonstrated that Si is beneficial for plant growth and development, especially under a wide range of abiotic stress conditions (Sanglard 2016; Shi *et al.* 2013; Yin *et al.* 2014). Si deposition occurs mainly as phytoliths (SiO_2_nH_2O) (Ye *et al.* 2013). It acts as a physical barrier and thus improves plant resistance to pathogens and insects. Najihah *et al.* (2015) observed that the accumulation of Si in epidermal and endodermal cell walls protected oil palm roots from penetration of *Ganoderma boninense* fungus. The objective of our study reported here is to determine the potential use of composted EFB as a source for the availability of Si to oil palm.

MATERIAL AND METHODS

Composting Technology

The experiment was carried out at Sungai Mirah Minting Estate, PT Bumitama Gunajaya Agro-Central Kalimantan. EFB materials were obtained from POM and chopped into 2.5-5.0 cm length. A four-week bio-decomposition process was employed by using a bio-decomposer containing *Trichoderma pseudokoningii*, *T. polysporum*, and *Phanerochaete chrysosporium*. In brief, composting steps involved EFB collection, shredding, mixing with bio-decomposer, incubation, and harvesting. Dosages of bio-decomposer were 0.2% (w/w) with four weeks incubation period without turning following the process outlined by Goenadi (2006).

Table 1. Chemical characteristics of fresh and composted EFB

Parameters	Fresh EFB	EFB compost
pH	6.3	8.0
N (%)	0.7	1.9
P_2O_5 (%)	0.4	0.6
K_2O (%)	2.5	3.8
SiO_2 (%)	11.3	28.7
dissolved Si (%)	0.03	0.44
Ca (%)	0.4	1.3
Mg (%)	0.3	0.58
CEC (cmol+/Kg)	7.3	52.1
C-organic (%)	41.9	36.9
C/N	59.9	19.4

Chemical Analysis

Analysis of EFB

The number of chemical characteristics of EFB before and after bio-decomposition was determined at the laboratory of IRIBB. The EFB samples were air-dried and passed through 100 mesh sieves and analyzed for the following: pH, nitrogen (Kjeldahl), phosphorus (spectrophotometer), potassium (Atomic Absorption Spectrophotometer, AAS), total SiO_2 (gravimetry), soluble Si (spectrophotometer), calcium (AAS), magnesium (AAS), cation exchange capacity (CEC) by using SNI 13-3494-1994 standard method, and C-organic (spectrophotometer).

Soil and leaf analysis

Soil samples were air-dried and passed through 2 mm sieve and analyzed for the following: pH, soil texture, C-organic, nitrogen, phosphorus, potassium, calcium carbonate, CEC, Boron, and exchangeable Al and H. Whereas leaf nutrient analysis was N, P, K, Mg, and SiO_2.

BioSilAc preparation

A 150 g of 325-mesh Belitung quartz sand sample was boiled in 100 mL HCl at 5 N concentrations until almost all of the solution evaporated to dissolve any contaminant elements present. The treated samples were then washed out with tap water several times to eliminate the contaminants and the rest of the HCl solution. Wet samples were transferred on a

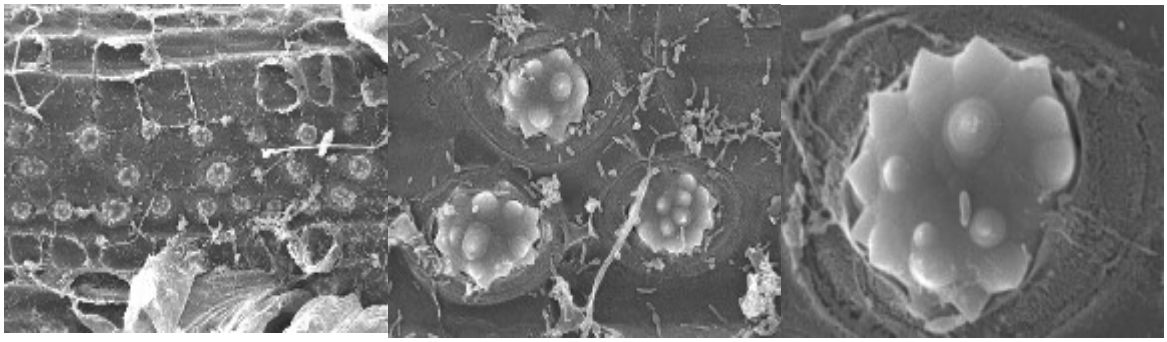

Figure 1. The silica body of fresh EFB found between fibre under microscopic magnification of 500x (left); 2,000x (middle); and 7,500x (right).

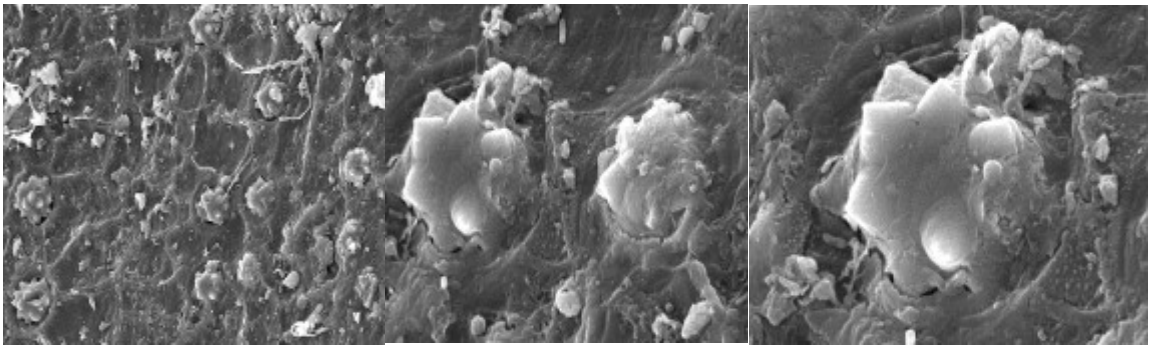

Figure 2. The silica body of EFB compost under microscopic magnification of 700x (left); 3,500x (middle); and 5,000x (right).

sheet of paper and dried out at 100°C in an oven until completely dry 60 g washed-sample was then mixed with 80 g NaOH (s) in a stainless pan and heated on the stove at 330°C while stirred manually until melted. The melted mixture was kept stirred until it dried out. After cooling at room temperature, 60 g pre-treated quartz sand was dissolved in 400 mL distilled water. The liquid obtained was the soluble silica (H_4SiO_4) (Santi *et al.* 2017), whereas the solid formula was prepared by the inoculation of acid-base-pretreated 325-mesh quartz sand with Si-solubilizing microbes i.e.: *Burkholderia cenocepacia*, *B. vietnamiensis*, *Aspergillus niger*, *Aeromonas punctata* (Santi & Goenadi, 2017). These two Si sources are called as BioSilAc. Silica concentration was determined by spectrophotometer.

Scanning Electron Microscopy Analysis

This analysis was performed to confirm the presence of Si in EFB tissues. All solid material of fresh and composted were examined with a Scanning Electron Microscope (SEM). A slice cut of EFB fiber was taken and prepared for SEM analyses. The electron beam is accelerated through a high voltage of 20 kV and passes through a system of apertures and electromagnetic lenses to produce a thin beam of electrons (Zhou *et al.* 2006). In the early stages, a material sample levelled with a special tool. After sputter coating the cast with 35 nm of gold-palladium (Au-Pd), electron micrographs were generated using a JeolJSM-5310LV SEM.

Field Experiment

A field experiment was conducted at Sungai Mirah Minting Estate, Central Kalimantan and arranged in seven treatments, i.e. combination of EFB compost and BioSilAc application with reduced dosages of NPK fertilizers, were arranged in a random block design with three replicates. The BioSilAc used was in liquid and solid forms. Soil chemical characteristics of immature-plant plot were pH 5.0; 83% sand; 14.5% clay; 2.5% silt; 0.12 (N); 1.98% (C-organic); 0.79 cmol+/kg (exchangeable Al); 0.32 cmol+/kg (exchangeable H); 3.67cmol+/kg CEC; 6.4 ppm (B); 0.006% (P_2O_5); 0.18% (K_2O); and 0.05% (CaO). The data from mature-plant plot were pH 4.8; 61.0% sand; 25.7% clay; 13.3% silt; 0.17 (N); 3.02% (C-organic); 1.4 cmol+/kg (exchangeable Al); 0.74 cmol+/kg (exchangeable H); 6.8 cmol+/kg CEC; 5.5 ppm (B); 0.102% (P_2O_5); 0.17% (K_2O); and 0.34% (CaO). Applied on a two-year (immature) and five-year (mature) old plants the treatments consist as follows: (i) 100% NPK standard dosage (T1); (ii) T1+ 225 kg BioSilAc /ha/year; (iii) 75% (T1) + 225 kg BioSilAc/ha/year; (iv) T1+ 4 L BioSilAc/ha/year; (v) 75% (T1) + 4 L BioSilAc/ha/year; (vi) T1 + 500 kg EFB compost + 2L BioSilAc/ha/year; (vii) 75% (T1) + 500 kg EFB compost + 2L BioSilAc/ha/year. The oil palm

Table 2. The leaf nutrient contents of immature oil palm one year after treatments.

Treatments	Leaf nutrient contents (%)				
	N	P	K	Mg	SiO_2
NPK 100% standarddosage (T1)	2.7	0.21	0.9	0.15	0.98
(T1) + 225 kg BioSilAc/ha/year	2.7	0.28	1.3	0.18	2.5
75% (T1) + 225 kg BioSilAc/ha/year	2.6	0.26	1.2	0.20	2.9
(T1) + 4 Liter BioSilAc/ha/year	2.7	0.24	1.0	0.18	1.04
75% (T1) + 4 Liter BioSilAc/ha/year	2.7	0.27	1.3	0.21	1.78
(T1) + 500 kg EFB compost + 2 L BioSilAc/ha/year	2.5	0.26	0.8	0.21	1.90
75% (T1) +500 kg EFB compost + 2 L BioSilAc/ha/year	2.7	0.27	1.0	0.20	1.10

Note: Classification of leaf nutrient contents of oil palm according to Fairhurst dan Hardter (2003): N (%) = <2.50 (deficient), 2.6-2.9 (optimum), >3.1 (high); P(%) = <0.15 (deficient), 0.16-0.19 (optimum), >0.25 (high); K (%) = <1.00 (deficient), 1.1-1.3 (optimum),> 1.8 (high); and Mg (%) = <0.20 (deficient), 0.30-0.45 (optimum), >0.70 (high).

plants were planted in 2013 (mature) and 2015 (immature). Each was applied on a plot consisting of 25 trees with nine of them in the middle as observed -trees. Selected parameters observed included leaf nutrient content (N, P, K, and Mg) of leaf no. 9, average weight and number of FFB. Data were analyzed by ANOVA and Duncan's Multiple Range Test (DMRT).

RESULTS AND DISCUSSION

Fresh and Composted EFB Chemical Characteristics

Chemical characterization of the fresh- and composted-EFB was conducted to determine the potential level of dissolved Si and other nutrients that can be utilized by plants. The characterization results are presented in Table 1. The results indicated that the levels of N, P, K, Ca, and Mg from the composted-EFB increased. Similarly, total SiO_2 and dissolved Si contents increased significantly, i.e. 2.5 and 14.6 times, respectively, in comparison to non-decomposed EFB. Furthermore, there was an increase in CEC and pH values, whereas the C/N ratio was decreased drastically from 59.9 to 19.4. Therefore, composting EFB with bio-decomposer for 28 days incubation has improved the quality of organic material, the nutrients content, and the availability of Si for plants.

The Present of Silica Body in EFB

In general, EFB has a thicker cell wall, thinner lumen, smaller diameter, and shorter fibers. EFB fibers have similar cell wall thickness and fiber length while having a thicker lumen and larger diameter when compared with hardwood species (Law *et al.* 2007; Jinn *et al.* 2015). The evidence of Si present in fresh and composted EFB was collected by using a scanning electron microscope (SEM). The SEM analysis showed that the amount of crystalline Si in the cross-sectional slices of EFB quite abundant in fresh (Figure 1) and composted EFB (Figure 2). Silica bodies were bind between the fibers. The silica bodies observed on fibre strands were a round-spiky shape. This evidence is in agreement with those reported by Harun *et al.* (2013) and Jinn *et al.* (2015). In composted EFB Si position nearly separated from fiber tissue because the tissue

Table 3. Growth of immature oil palm one year after treatments.

Treatments	Frond length (cm)	Number of leave (sheet)	Width of petiole (cm)	Dense of petiole (cm)
NPK 100% standarddosage (T1)	340.3^{ab}	218^{ab}	4.9^{ab}	3.2^{a}
(T1) + 225 kg BioSilAc/ha/year	328.0^{b}	211^{b}	4.9^{ab}	3.0^{ab}
75% (T1) + 225 kg BioSilAc/ha/year	372.8^{a}	208^{b}	5.2^{a}	3.3^{a}
(T1) + 4 Liter BioSilAc/ha/year	354.6^{ab}	230^{ab}	4.2^{c}	2.5^{b}
75% (T1) + 4 Liter BioSilAc/ha/year	320.9^{b}	251^{a}	4.3^{bc}	2.4^{b}
(T1) + 500 kg EFB compost + 2 L BioSilAc/ha/year	342.9^{ab}	239^{ab}	4.7^{abc}	2.9^{ab}
75% (T1) +500 kg EFB compost + 2 L BioSilAc/ ha/year	383.2^{a}	223^{ab}	5.4^{a}	3.6^{a}
Coefficient variable (%)	6.6	7.7	8.0	11.4

Note: Values in the same column followed by the same superscript letter(s) are not significantly different according to Duncan's Multiple Range Test (P<0.05).

Table 4. The productivity of 2013 planting year oil palm, one year after treatments.

Treatments	Number of FFB	Average weight of FFB (kg)	FFB production (ton/ha/year)
NPK 100% standarddosage (T1)	1,823^{bc}	4.83^{a}	8.80^{ab}
(T1) + 225 kg BioSilAc/ha/year	1,750^{c}	4.70^{b}	8.23^{c}
75% (T1) + 225 kg BioSilAc/ha/year	1,800^{c}	4.70^{b}	8.47^{bc}
(T1) + 4 Liter BioSilAc/ha/year	1,889^{bc}	4.50^{c}	8.50^{a}
75% (T1) + 4 Liter BioSilAc/ha/year	1,973^{ab}	4.63^{b}	9.13^{a}
(T1) + 500 kg EFB compost + 2 L BioSilAc/ha/year	1,875^{bc}	4.70^{b}	8.80^{ab}
75% (T1) +500 kg EFB compost + 2 L BioSilAc/ ha/year	2,084^{a}	4.70^{b}	9.23^{a}
Coefficient variable (%)	4.6	1.4	2.9

Note: Values in the same column, followed by the same superscript letter(s) are not significantly different according to Duncan's Multiple Range Test (P<0.05).

conditions of EFB has become weak. The structure of composted EFB tissue was somewhat fragile that enables the release of silica from these tissues will become easier.

Field Experiment

The first application of EFB compost and BioSilAc was conducted in January 2017. The data from this experiment showed that the application of EFB compost and BioSilAc after one year on an immature oil palm could maintain P, K, Mg, and Si absorptions better than those of other treatments including normal dosage of NPK fertilizer. When applied in combination with 500 kg EFB compost + 2 L BioSilAc/ha/year, they reduced the rate of NPK up to 75% standard dosage. Leaf P, K, and Mg content of 500 kg EFB compost combined with 75% NPK dosages were considered to be optimum, i.e.28.6% (P); 11.1% (K); 33.3% (Mg); and 12.2% (SiO_2) compared to the standard NPK dosage treatment. Meanwhile, data analyses indicated that total P content was relatively high (0.27%), whereas N, K, and Mg content of leaf among treatment plots of BioSilAc was at an optimum level according to the classification made by Fairhurst & Hardter (2003) (Table 2). Furthermore, application EFB compost and BioSilAc increased SiO_2 content on the leaf of immature oil palm. Application of 500kg EFB compost + 2 L BioSilAc combined with 75% dosage of NPK resulted in significantly higher vegetative growth of frond length, width and dense of petiole than those of other treatments (Table 3).

Table 4 presents the effect of treatments on the yield of a five-year-old palm. It is evidenced that the highest yield average in terms of FFB was obtained from the application of a 75% dosage of NPK combined with 500 kg EFB compost + 2 L BioSilAc/ha/year. The application of these treatments resulted in higher yield (than that obtained from 100% standard dosage of NPK. This study revealed that the use of EFB compost reduced the need of Si up to 50% for both immature and mature oil palms which promote both better vegetative and productive performances of the palm.

Table 5. Soil characteristics determined at one year after treatments on mature plant plots.

Treatments	pH H_20	N (%)	P_2O_5 (%)	K_2O (%)	C_{org} (%)	Al (%)	exchangeable Al ($cmol^+kg^{-1}$)
NPK 100% standarddosage (T1)	4.9^{a}	0.13^{d}	0.05^{b}	0.01^{c}	2.5^{b}	0.11^{ab}	1.50^{bc}
(T1) + 225 kg BioSilAc/ha/year	4.4^{de}	0.16^{bc}	0.01^{c}	0.03^{a}	2.6^{b}	0.06^{d}	1.81^{b}
75% (T1) + 225 kg BioSilAc/ha/year	4.7^{bc}	0.08^{e}	0.02^{c}	0.01^{c}	1.3^{c}	0.06^{d}	1.36^{c}
(T1) + 4 Liter BioSilAc/ha/year	4.4^{de}	0.18^{ab}	0.02^{c}	0.007^{cd}	2.9^{a}	0.10^{abc}	2.67^{a}
75% (T1) + 4 Liter BioSilAc/ha/year	4.5^{de}	0.19^{a}	0.08^{a}	0.01^{c}	3.1^{a}	0.12^{a}	1.74^{b}
(T1) + 500 kg EFB compost + 2 L BioSi-lAc/ha/year	4.7^{b}	0.08^{e}	0.04^{c}	0.004^{d}	1.2^{c}	0.10^{abc}	1.71^{b}
75% (T1) +500 kg EFB compost + 2 L BioSilAc/ha/year	4.6^{cd}	0.15^{cd}	0.06^{b}	0.02^{b}	2.9^{a}	0.09^{c}	1.21^{c}
Coefficient variable (%)	1.2	7.0	19.2	14.4	4.0	9.6	7.7

Notes: Figures in the same column followed by the same letter(s) are not significantly different according to Duncan's Multiple Range Test (P<0.05).

The effect of treatments on selected soil chemical properties after one year of application is shown in Table 5. In general, the selected chemical properties of the soil were not so much different among those treatments. No clear evidence noticed or shown relationships between Si application and P and Al contents. However, it is observed that in general application of Si tended to decrease the Al content in the soil. Britez *et al.* (2002) reported that silicon (Si) can make stable complexes with Al and reduce the harmful Al effects. Si can potentially increase the root elongation rate (RER) in Al-toxic solutions, with the magnitude of the effect increasing with the concentration of Si (Koppittke *et al.* 2017). Moreover, these researchers also confirmed that Si is not only deactivated Al in the rhizosphere but also in plant shoot tissue avoiding Al toxicity to the plant.

CONCLUSIONS

The application of Si (BioSilAc) improved the vegetative performance of immature and yield of mature oil palm (4.9%) and increased NPK fertilizer use efficiency (25%) one year after treatment. A 28-day bio-composted EFB could provide Si available to the plant and the addition of 500 kg EFB compost/ha/year combined with 75% NPK fertilizer reduced 50% the need for BioSilAc. Further research is needed to evaluate the long-term effect of Si application on the yield of oil palm.

ACKNOWLEDGEMENTS

We would like to extend our sincere gratitude to The Indonesia Estate Crop Fund Management Agency for Palm Oil, for valuable supports in funding this research (Contract No. PRJ - 52 /DPKS/2016) and PT Bumitama Gunajaya Agro, for their kind co-operation in the field implementation project and logistical support.

REFERENCES

Britez, R.M, Watanabe T, Jansen S, Reissmann C.B, &Osaki M. 2002, The relationship between aluminium and silicon accumulation in leaves of *Faramea marginata* (Rubiaceae). *New Phytologist* 156, 437–444.

Epstein, E. 1994, The anomaly of silicon in plant biology. Proc. Natl. Acad. Sci. USA 91, 11–17.

Epstein, E. 2009, Silicon: Its manifold roles in plants. *Ann. Appl. Biol.* 155, 155–160.

Fairhurst, T. & Hardter, R.2003, Management for large and sustainable yields. Potash and Phosphate Institute of Canada. 382p.

Geng, A. 2013, Conversion of oil palm empty fruit bunch to biofuels. In: Fang Z (ed) Book of liquid, gaseous and solid biofuels—conversion techniques. Tech Open, Croatia.

Goenadi, D.H. 2006, Developing Technology for Biodecomposition of fresh solid wastes of plantation crops under tropical conditions. IPB Press.

Gunawan, F.E., Homma H, Brodjonegoro, S.S, Baseri-Hudin A, &Zainuddin A. 2009, Mechanical properties of oil palm empty fruit bunch fiber. *J Solid Mech Mater Eng,* 3(7), 943–951.

Harun, N.A.F., Baharuddin, A.S, Zainudin, M.H.M, Bahrin, E.K, Naim M.N, &Zakaria, R. 2013, Cellulose production from treated oil palm empty fruit bunch degradation by locally isolated Thermobifidafusca. *Bioresources,* 8(1), 676 – 687.

Jinn, C.M., H'ng P.S, Chin K.L., Chai E.W., Paridah M.T., Lee S.H., Lum W.C., Luqman C., &Mariusz, M. 2015, Agricultural biomass based potential materials. *In* Empty Fruit Bunches in the Race for Energy, Biochemical, and Material Industry. Springer International Publishing Switzerland. K. R. Hakeem (eds.).375-389 p.

Keeping, M.G.&Reynolds, O.L. 2009, Silicon in agriculture: New insights, new significance, and growing application.*Ann. Appl. Biol.* 155, 153–154.

Koppittke, P.M., ____Gianoncelli A., Kourousias G., Green K. & McKenna, B.A. 2017, Alleviation of Al toxicity by Si is associated with the formation of Al–Si complexes in root tissues of sorghum. *Frontiers in plant science*, 8: 1 -9.

Law, K.N., Daud, W.R. & Ghazali A. 2007, Morphological and chemical nature of fiber strands of oil palm empty-fruit-bunch (OPEFB). *Bioresource Technology,* 2(3),351-362.

Ma, J.F. 2004, Role of silicon in enhancing the resistance of plants to biotic and abiotic stresses. *Soil Science and Plant Nutrition,*50(1), 11 –18.

Ma J.F. &Yamaji N.A. 2015, Cooperative system of silicon transport in plants. *Trends Plant Sci,* 20, 435–442.

MaJ.F, Tamai K, Ichii M. & Wu G.F. 2002, A Rice Mutant Defective in Si Uptake. *Plant Physiol,* 130, 2111–2117.

Mitani N, & Ma J.F. 2005, Uptake system of silicon in different plant species. *J. Exp. Bot,* 56, 1255 –1261.

Montpetit J., Vivancos J., Mitani-Ueno N., Yamaji N., Rémus-BorelW., Belzile F., Ma J.F., & Bélanger R.R. 2012, Cloning, functional characterization and heterologous expression of TaLsi1, a wheat silicon transporter gene.*Plant Mol. Biol,* 79, 35–46.

Najihah, N.I, Hanafi, M.M, Idris, A.S. & Hakim, M.A. 2015, Silicon treatment in oil palms confers resistance to basal stem rot disease caused by Ganoderma boninense. *Crop Prot,* 67, 151–159.

Sanglard, L.M.V.P, Detmann, K.C, Martins, S.C.V, Teixeira, R.A, Pereira, L.F, Sanglard, M.L, Fernie, A.R, Araújo, W.L. & DaMatta, F.M. 2016, The role of silicon in metabolic acclimation of rice plants challenged with arsenic.*Environ. Exp. Bot,* 123, 22–36.

Santi, L.P,&Goenadi, D.H. 2017, Solubilization of silicatefrom quartz mineral by potential silicate solubilizing bacteria. *Menara Perkebunan,* 85(2), 96-105.

Santi, L.P, Mulyanto D., &Goenadi, D.H. 2017, Double acid-base extraction of silicic acid from quartz sand. *Journal of Minerals and Materials Characterization and Engineering*, 5(6), 362-373.

Shi, Y., Wang Y., Flowers, T.J.&Gong, H. 2013, Silicon decreases chloride transport in rice (*Oryza sativa* L.) in saline conditions. *J. Plant Physiol,* 170, 847–853.

Standar Nasional Indonesia (SNI). 1994, Mineral zeolit, Pengukuran kapasitas pertukaran kation. 13-3494-1994.

Vivancos, J., Labbé C., Menzies, J.G.&Bélanger, R.R. 2015, Silicon-mediated resistance of Arabidopsis against powdery mildew involves mechanisms other than the salicylic acid (SA)-dependent defence pathway.*Mol. Plant Pathol,* 16, 572–582.

Yin, L., Wang S., Liu P., Wang W., Cao D., Deng X.&Zhang S. 2014, Silicon-mediated changes inpolyamine and 1-aminocyclopropane-1-carboxylic acid are involved in silicon-induced drought resistance in Sorghum utilized L. *Plant Physiol. Biochem,* 80, 268–277.

Ye, M., Song Y., Long J.W.R., Baerson, S.R., Pan Z, Zhu-Salzman, K., Xie J., Cai K.&Luo S. 2013, Priming of jasmonate-mediated antiherbivore defense responses in rice by silicon. *Proc. Natl. Acad. Sci,* USA 110, E3631–E3639.

Zhou, W., Apkarian R., Wang, Z.L. &Joy, D. 2006, Fundamentals of ScanningElectron Microscopy (SEM). In: Zhou W. & Wang Z.L, Eds., Scanning Microscopy for Nanotechnology Techniques and Applications, Springer Science BusinessMedia, New York.

Journal of Tropical Biodiversity and Biotechnology
Volume 04, Issue 03 (2019): 97 — 106
DOI: 10.22146/jtbb.45667

Research Article

Antlers Characterization for Identification of Deer Species (Family Cervidae) in Indonesia

Donan Satria Yudha[1], Muhammad Zulfiqar Meizar Pratama[2]*, Rury Eprilurahman[1]

1) Laboratory of Animal Systematics, Faculty of Biology, Universitas Gadjah Mada, Yogyakarta. Jl. Teknika Selatan Sekip Utara Yogyakarta, 55281
2) Faculty of Biology, Universitas Gadjah Mada, Yogyakarta. Jl. Teknika Selatan Sekip Utara Yogyakarta, 55281

*Corresponding author, tel.: +62 82136900891, email address: zulfiqar285@ymail.com

Keywords:
deer
antler
characterization
identification
Indonesia

Article history:
Submitted 08/05/2019
Revised 13/09/2019
Accepted 25/09/2019

ABSTRACT

There are five species of deer (family Cervidae) living in Indonesia today. Male deer possesses antlers, a unique character of male deer. Antlers have economic values for quite a long time. Antler's growth is influenced by several factors, therefore each species of deer have its own unique antlers' shape and size. Antler's identification usually relies on size measurement and overall shape of complete antlers which still attach to the skull. It is difficult to identify shed, broken or individual antler. The purpose of the research is to understand antlers' morphological characters on each species to become diagnostic characters. Specimens analysed were collections of LIPI and were analysed with Principal Component Analysis (PCA) using PAST3 software. The results showed each species of deer having their own unique antlers' character, and so it can be used to determine the species of Indonesian deer. The important structures for identification are relief, pedicle, brow, *bez*, and main beam.

INTRODUCTION

Deer or cervids (family Cervidae) is one of the families in the Artiodactyl groups which is second most diverse member after bovids (family Bovidae) (Prothero & Foss, 2007). Five valid species of cervids are living and naturally distributed in Indonesia, they are: *Rusa timorensis* (Javan rusa or Sunda sambar), *Rusa unicolor* (Sambar), *Axis kuhlii* (Bawean deer), *Muntiacus muntjak* (Indian muntjac, southern red muntjac, barking deer) and *Muntiacus atherodes* (Bornean yellow muntjac). *Muntiacus montanus* from Sumatra might be another species of deer in Indonesia, but not enough data had been collected to evaluate the validity of this species. Furthermore, there is one introduced species which is *Axis axis* (chital, spotted deer or axis deer) (Goss, 1985; Bubenik & Bubenik, 1990; Stefoff, 2008; Timmins *et al.*, 2016).

One of the characteristics of deer is antlers on individual male. Antlers are frontal bone which grow outwards from frontal skull and usually called *pedicle* (Price *et al.*, 2005). The development of antlers is influenced by several factors, among them are: age, nutrition, and genetics. Consequently, each species of deer forms specific antlers with specific size and shape (Heffelfinger 2006).

Antlers attract human since ancient time. Most of antlers were trade as trophy and displayed on the wall. Some of it was processed into aphrodisiac or as traditional medicine; however the efficacy is not scientifically proven yet (Walrod, 2010). Species identification of deer using antlers commonly based on the size and shape of the complete antlers which still attach to the skull (CITES, 2003). Some antlers were traded separately or individually without its skull, therefore it's difficult to determine the species origin.

Four of the native deer species in Indonesia are an endemic species, i.e. *Rusa timorensis*, *Axis kuhlii*, *Muntiacus atherodes*, and *Muntiacus montanus*. Rusa timorensis and *Rusa unicolor* are considered vulnerable by the IUCN Red list, while *Axis kuhlii* is considered critically endangered. All the native deer species of Indonesia is protected by the Indonesian Government Regulation (2018), except for *Muntiacus montanus* which couldn't be evaluated yet. Even though the deer of Indonesia are protected by the law, some illegal hunting and antlers poaching is still

happening in some places (Hedges *et al.*, 2015; Semiadi *et al.*, 2015; Timmins *et al.*, 2016a, 2016b). An accurate way to identify antlers is needed to help enforcing the law.

The purpose of this research is to identify antlers' morphological characters on each species to be a diagnostic character. These diagnostic characters can be an alternative of species identification. The results were expected to assist the species identification of antlers found without its skull in trade market or fossils.

MATERIALS AND METHODS

Materials

Materials used are deer antlers collection of the Laboratory of Mammals Biosystematics, Museum Zoologicum Bogoriense (MZB), Research Center for Biology–Indonesian Institute of Sciences (LIPI). Data were collected from 88 specimens; 86 of them were antlers that are still intact with the skull. There are 30 antlers of *Muntiacus muntjak* (15 skulls), 2 antlers of *Axis axis* (1 skull), 8 antlers of *Axis kuhlii* (4 skulls), 12 antlers of *Rusa unicolor* (6 skulls), and 36 antlers of *Rusa timorensis* (17 skulls and 2 shed antlers). A complete antler commonly consists of a *pedicle*, *burr*, *base*, *main beam*, *brow* and *bez* (Figure 1).

Methods

The methods used was morphological comparison of antlers characteristics and morphometric analysis based on Boone & Crockett Club (1887) and Semiadi *et al.* (2003). The morphological and morphometric data acquired were then analysed using Principal Component Analysis (PCA) with *software* PAST3. PCA analysis was conducted to exemine characters grouping in order to determine its diagnostic characters. The characters used in this research are shown on Table 1.

Antler's relief is determined from five categories. Smooth for antlers with no relief. Faint for antlers with visible relief striation but couldn't be felt by touch. Weak for antlers with visible striation and could be slightly felt by touch. Strong for antlers with visible thick relief striation and could be felt by touch. Pearled for antlers with strong relief and pearly structure.

RESULTS AND DISCUSSION

Antlers' morphological characters

There are characters which are diagnostic of each taxa. Some characters are qualitative and the rest are binary ("present" or "absent"; value "1" or "0"). Those characters are shown on Table 1. Some characters on Table 1, can only be measured if the antlers are still intact with the skull. Characters which need intact condition are: B (distance between tips of main beams), C (greatest distance between both antlers), and D (greatest distance between both main beam's inner side). Those characters should be considered when identifying antlers, however it couldn't assist to identify shed, broken and individual antlers.

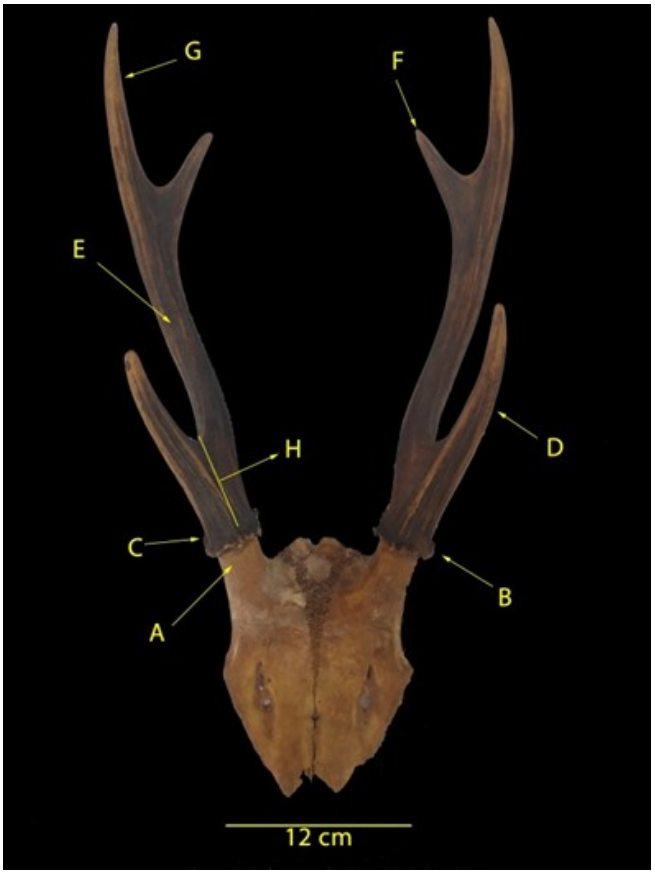

Figure 1. Antlers' main part which are observed: A. Pedicle, B. Burr, C. Base, D. Brow, E. Main beam 2nd segment, F. Bez, G. Main beam 3rd segment, H. BeHt (distance of bez branching to the base), I. BrHt (distance of brow branching to the base).

Accessory on an antler is usually not the main character for identification. Accessories are usually just an abnormal growth of an antler. Therefore, the presence of accessories should not be the main consideration as a diagnostic character.

Diameter, perimeter, and length can be quite significant characters for antler's identification. Nevertheless, along with those characters, other characters should also be considered when identifying antlers. Antler's diameter and perimeter will also increases along with the pedicle growth. Pedicle will grow along with the skull's growth, meaning when an animal age increase, the size will also increases. Each species of deer have their own unique range of size, hence those characters could

Table 1. Variation of antlers characteristics which can be diagnostic characters

No	Code	Characters		Data type
1	Re	Reliefs	Smooth Faint Weak Strong Pearled	Level
2	PDt	Transversal diameter of pedicle		Nominal
3	Pdap	Anteroposterior diameter of pedicle		Nominal
4	PP	Perimeter of pedicle		Nominal
5	BuDt	Transversal diameter of *burr*		Nominal
6	BuDap	Anteroposterior diameter of *burr*		Nominal
7	BuP	Perimeter of *burr*		Nominal
8	BDt	Transversal diameter of base		Nominal
9	Bdap	Anteroposterior diameter of base		Nominal
10	BP	Perimeter of base		Nominal
11	M2P	Perimeter of 2nd beam segment		Nominal
12	M2Dt	Transversal diameter of 2nd beam segment		Nominal
13	M2Dap	Anteroposterior diameter of 2nd beam segment		Nominal
14	M3P	Perimeter of 3rd beam segment		Nominal
15	M3Dt	Transversal diameter of 3rd beam segment		Nominal
16	M3Dap	Anteroposterior diameter of 3rd beam segment		Nominal
17	ML	Main beam length		Nominal
18	BrDt	Transversal diameter of brow		Nominal
19	BrDap	Anteroposterior diameter of brow		Nominal
20	BrP	Perimeter of brow		Nominal
21	BrHt	Brow branching distance to base		Nominal
22	BrAng	Brow branching angle		Nominal
23	BrL	Brow length		Nominal
24	Be	Presencce of *bez*		Binary
25	BeDt	Transversal diameter of *bez*		Nominal
26	BeDap	Anteroposterior diameter of *bez*		Nominal
27	BeP	Perimeter of *bez*		Nominal
28	BeHt	*Bez* branching distance to base		Nominal
29	BeAng	*Bez* branching angle		Nominal
30	BeL	*Bez* length		Nominal
31	B	Distance between the tips of main beams		Nominal
32	C	Greatest distance between both antlers		Nominal
33	D	Greatest distance between both main beam's inner side		Nominal
34	PFl	Flattened pedicle		Binary
35	M2Flb	Laterolaterally flattened 2nd segment of main beam		Binary
36	BrFla	Anteroposteriorly flattened brow		Binary
37	BrFlb	Laterolaterally flattened brow		Binary
38	BrPa	Brow parallels to main beam		Binary
39	BeMed	*Bez* grow inward		Binary
40	BeLat	*Bez* grow outward		Binary
41	AcH1	Accessory on branching of brow		Binary
42	AcBr	Accessory on brow		Binary
43	AcM2	Accessory on 2nd segment of main beam		Binary
44	AcBe	Accessory on *bez*		Binary

also be considered as diagnostic characters. The length of antlers could vary during growth cycle of antler. Old deer could also have a short antler if that antler had just regrown after being shed at the previous cycle. Besides that, in some cases, antlers could also be broken when two males are fighting each other on mating season or when it's attacked by other animals, including by humans (McPherson & McPherson 2008). Therefore, the full length of the antlers couldn't be measured on some specimens.

Antler specimens of Indonesian deer

Principal Component Analysis was conducted from the data collected. The correlation analysis between group results in eigenvalues and percent variances shown in Table 2, while the scatter plot can be seen in Figure 2 as follows.

The results shown in Figure 2, were the data of antlers analysed in which the antlers were not attached to the skull anymore. Some characters i.e. B (tip to tip distance), C (greatest distance between both antlers), and D (greatest distance between both antlers' inner side) is not included in that PCA due to isolated antlers. The antlers analysed in Figure 2 were only one side and not attached to the skull, therefore it is impossible to measure. Some groups show wide range in the PCA scatter plot, it indicates variance on the characters. This was caused by the difference in condition of the antlers used in analysis. Some specimens was just started its adult stage which was indicated by the size of the skull and mainly its pedicle, meanwhile some specimens have reached its maximal size. Some antlers undergo abnormality in its growth which altered the antler's proportion. Nevertheless, each species group could be shown on the scatter plot and have a quite significant distance between each other. The loading plot of component 1 can be seen as follows on Figure 3, while the loading plot of component 2 can be seen on Figure 4.

Table 2. Eigenvalue and % Variance

PC	Eigenvalue	% Variance
1	24.1244	73.104
2	4.83482	14.651
3	2.55828	7.7524
4	1.48246	4.4923

The *Muntiacus muntjak* group is separated by a great distance from the other groups (Figure 2). This grouping is supported by some characters, namely BrFla (brow flattened anteroposteriorly), PFl (pedicle flattened laterolaterally), and M2Flb (2nd segment of main beam flattened laterolaterally). *Muntiacus muntjak* have a long and flattened pedicle, meanwhile the other species of deer in Indonesia have short and rounded pedicles. The brows are flattened antero-posteriorly. The second segment of main beam is flattened latero-laterally, especially on its tip (Figure 5). Besides that, it is shown in the Figure 2 that bez characters points away from the *Muntiacus muntjak* group.

The antlers of *Muntiacus* doesn't have *bez*, hence the *bez* character in the *Muntiacus muntjak* group will always be 0. The absence of bez is a significant character to differentiate *Muntiacus* with the other groups of deer in Indonesia (Figure 5).

In Indonesia, *Muntiacus* genus is not only represented by *Muntiacus muntjak*, but also *Muntiacus atherodes*. In LIPI, there is no antler collection of *Muntiacus atherodes*, therefore analysis couldn't be done to differentiate between the antlers of *Muntiacus muntjak* and *Muntiacus atherodes*.

The *Axis* group is scattered in the lower quadrant (Figure 2). It is shown that the characters which support this group are BeMed (*bez* grows inward) and BrPa (brow parallel to main beam). All of the species in the *Axis* genus in Indonesia have *bez* that grow inward (Figure 6). This character is also present in *Rusa unicolor*. *Axis* group tend to have brows which grow parallel to the main beam. Re (relief) character on the scatter plot points away from the *Axis* group. Compared to the other deer groups in Indonesia (represented on Figure 2), genus *Axis* have antlers with a relatively weak relief. Genus *Axis* also has cylindrical and slim antlers, meanwhile the *Muntiacus* have a flattened short antlers (shown in Figure 5) and the *Rusa* have a large rugose antlers (see Figure 7 and 8).

On the scatter plot in Figure 2, *Axis axis* groups located on the outer edge of *Axis kuhlii*'s groups. The fewer numbers of *Axis axis* specimen available for analysis may result in an unfavourable grouping on the scatter plot. *Axis axis* is not a native animal in Indonesia. *Axis axis* in Indonesia was introduced from the middle Asia (Stefoff, 2008). *Axis axis* in Indonesia could only be found in the manmade areas, such as the Bogor Palace (Istana Bogor) and zoos. Therefore, the specimens obtained were in low numbers.

Generally, *Axis axis* antler's is longer than *Axis kuhlii*'s. Furthermore, the antlers of *Axis axis* have *bez* that tends to grow slightly upwards (forming a U-shape), meanwhile in *Axis kuhlii* it tends to grow straight (forming an L-shape) (Figure 7).

The group of genus *Rusa* is scattered on the right side of the quadrant (Figure 2). Characters which support this grouping are diameter and circumference of antlers. Compares to the other groups, genus *Rusa* generally have a bigger antler.

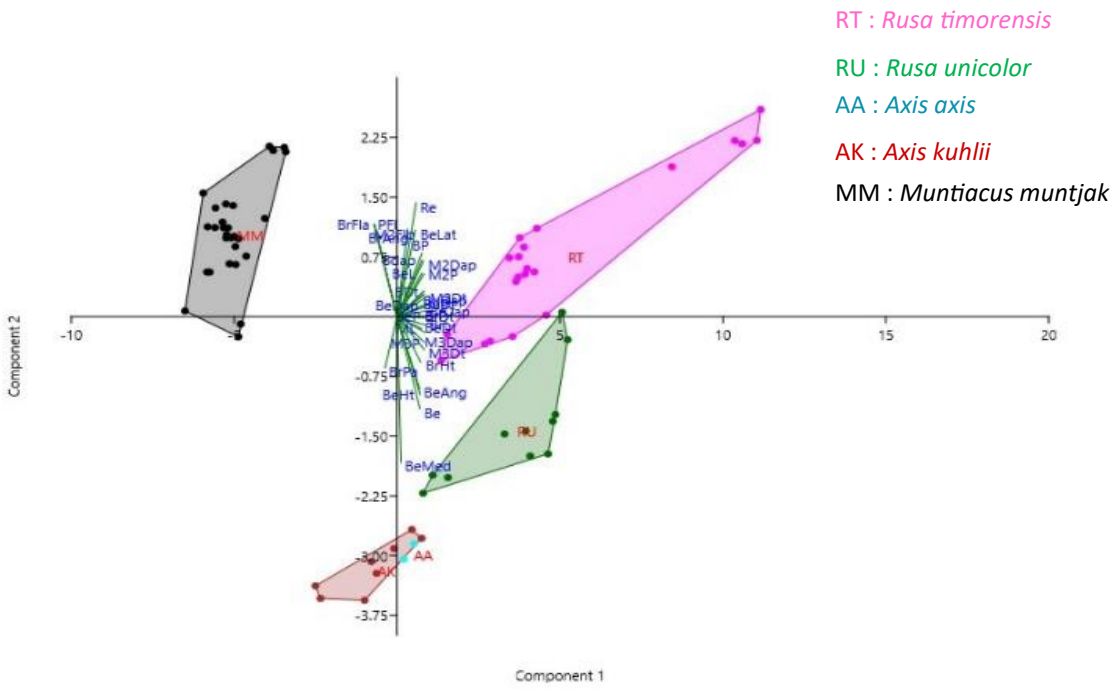

Figure 2. The PCA results of individual antlers.

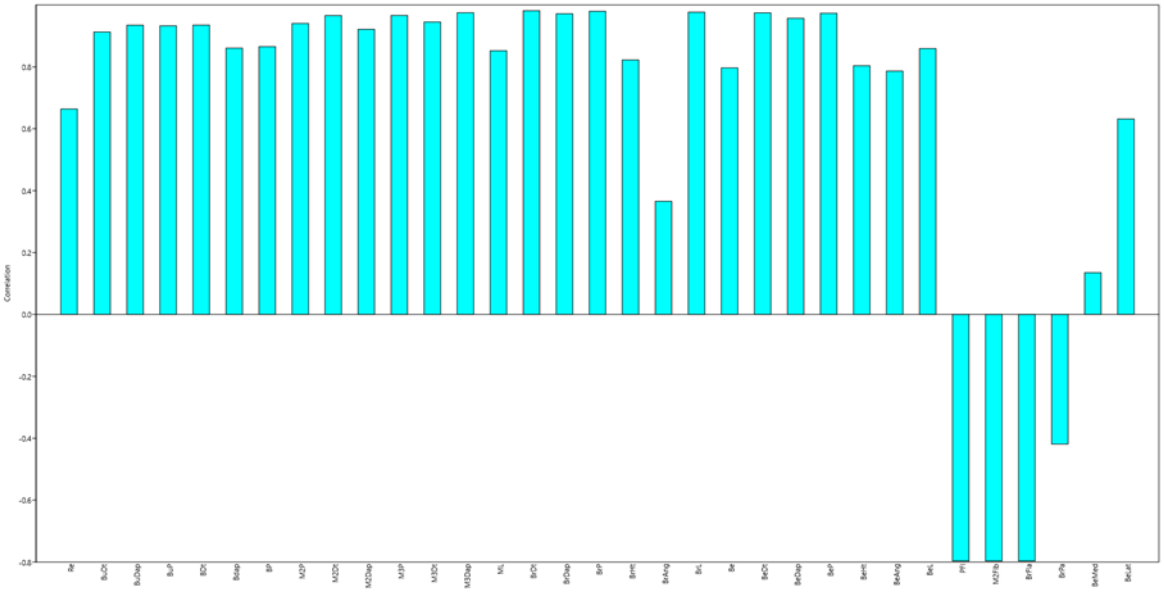

Figure 3. The loading plot of component 1

Rusa unicolor's group is supported by some characters, which are: the combination of BeAng (*bez* branching angle), BeHt (distance of *bez* branching to base), BrHt (distance of *bez* branching to base), also characters of the diameter and circumference which generally support the *Rusa* group. *Rusa unicolor* can be differentiated from *Rusa timorensis* by some characters, especially BeMed (*bez* grows inward), where *Rusa unicolor* have *bez* that grow inward just like those in *Axis kuhlii*. *Bez* of *Rusa unicolor*'s antlers also tend to grow straight just like *Axis kuhlii*'s, but they can be differentiated by some characters. *Rusa unicolor* have higher BrHt value, while *Axis kuhlii* have lower BrHt value. *Rusa unicolor*'s antlers also have stronger relief than *Axis kuhlii*'s, *Rusa unicolor* also have larger *bez* while *Axis kuhlii*'s are relatively slender (Figure 8).

Rusa timorensis group is supported by some characters, namely Re (relief), BeLat (*bez* grows outward), M2Dap (anteroposterior diameter of main beam's 2nd segment), BP (perimeter of base), and M2P (perimeter of main beam's 2nd segment). *Rusa timorensis*'s antlers tend to have pearled relief. Among

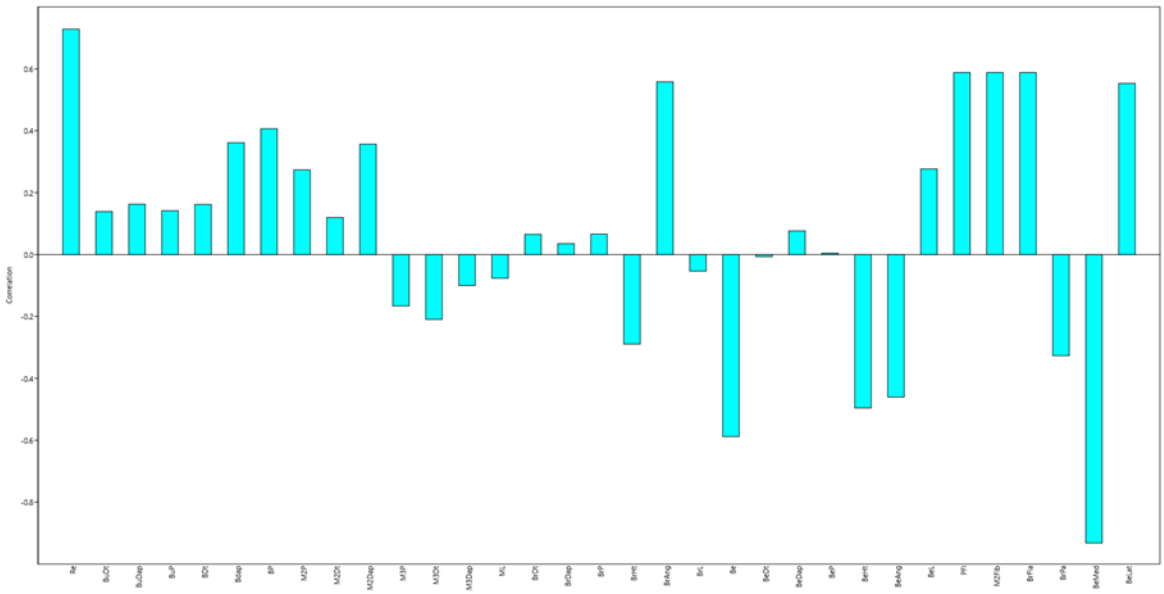

Figure 4. The loading plot of component 2

Indonesian deer, *Rusa timorensis* is the only one whose *bez* grows outward (represented on Figure 2).

Figure 5. *Muntiacus muntjak* specimen, left: dorsal view and right: lateral view, with description: A. Pedicle, B. Burr, C. Brow, D. 2nd segment of main beam.

PCA results on Figure 10 was an analysis of paired antlers. In this analysis, character B (tip to tip distance), C (greatest distance between antler), and D (greatest distance of main beam's inner side) was included in the analysis. By including B, C, and D characters, some changes can be seen on the scatter plot shown on figure 10. The eigenvalue and % variance is shown on Table 3.

On the *Axis* group (Figure 10), changes can be seen that the *Axis axis's* and *Axis kuhlii*'s group become distinctly separated. *Axis axis's* antlers tend to spread widely, where *Axis kuhlii*'s tend to grow upward. This causes the distance between antlers in *Axis axis* to be wider than those of *Axis kuhlii*'s, hence *Axis axis* have greater value of B, C, and D. On larger specimens (which couldn't be found in LIPI's collection), *Axis axis*'s antlers grows significantly wider than shown in the PCA result (see Figure 11).

Table 3. Eigenvalue and % Variance of paired antler specimens' PCA

PC	Eigenvalue	% variance
1	28.3827	72.776
2	5.29825	13.585
3	3.10356	7.9579
4	2.21546	5.6807

On the *Rusa* group (Figure 10), changes occur by which the groups become more clumped together. The changes happen because in the *Rusa* group, the specimens used were highly varied in terms of their ages and phases in the growth cycle; hence the variance of size is high. While the sizes vary highly between age groups, the distance between antlers tend to be the same, hence the low variance of distance between antlers' characters makes the scatter plot become more clumped. The distance between *Rusa timorensis's* and *Rusa unicolor*'s group also decreases. This was caused by the relatively equal antlers' average circumference and diameters of both species.

It should also be noted that in its growth,

Figure 6. Comparison of *Muntiacus muntjak* and *Rusa unicolor* antlers. *Muntiacus muntjak* antlers don't have *bez*.

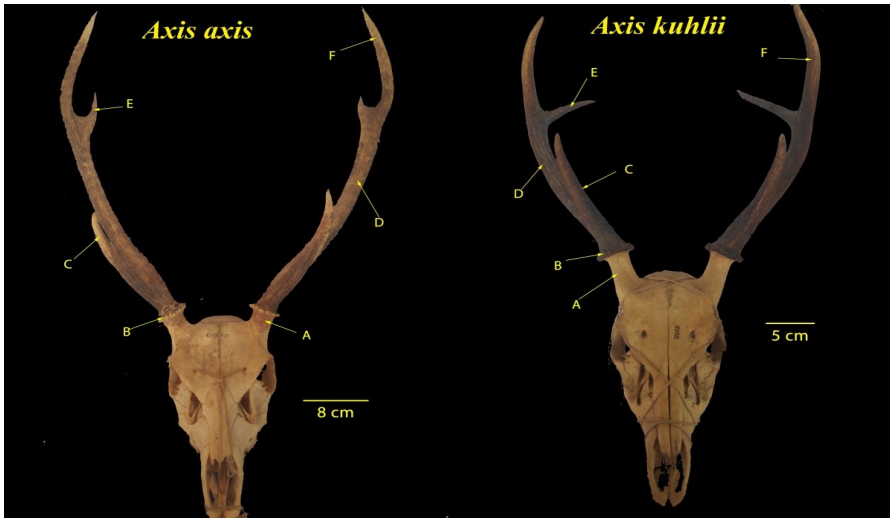

Figure 7. Specimens of *Axis* group: *Axis axis* (left) and *Axis kuhlii* (right), with description: A. Pedicle, B. Burr, C. Brow, D. 2nd segment of main beam, E. Bez, F. 3rd segment of main beam.

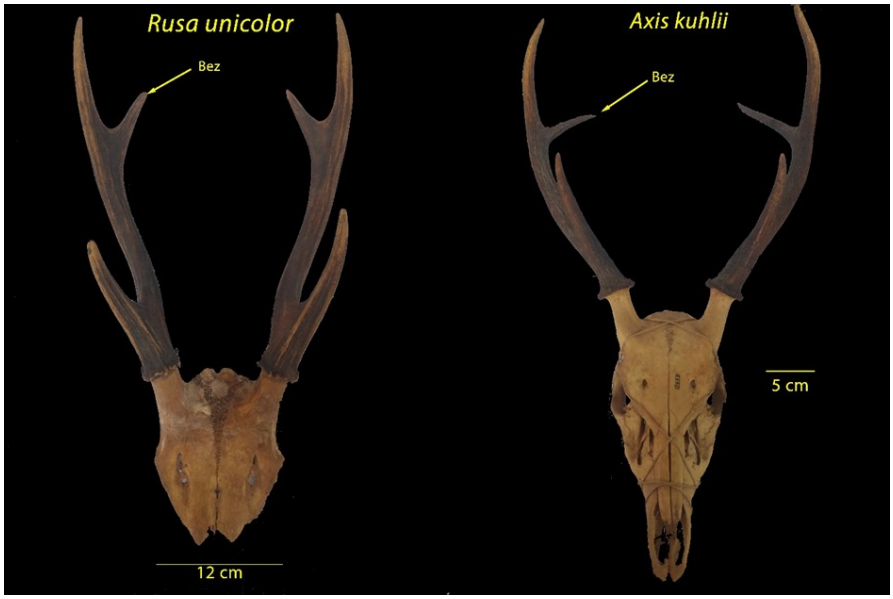

Figure 8. Antler comparison of *Rusa unicolor* (left) and *Axis kuhlii* (right).

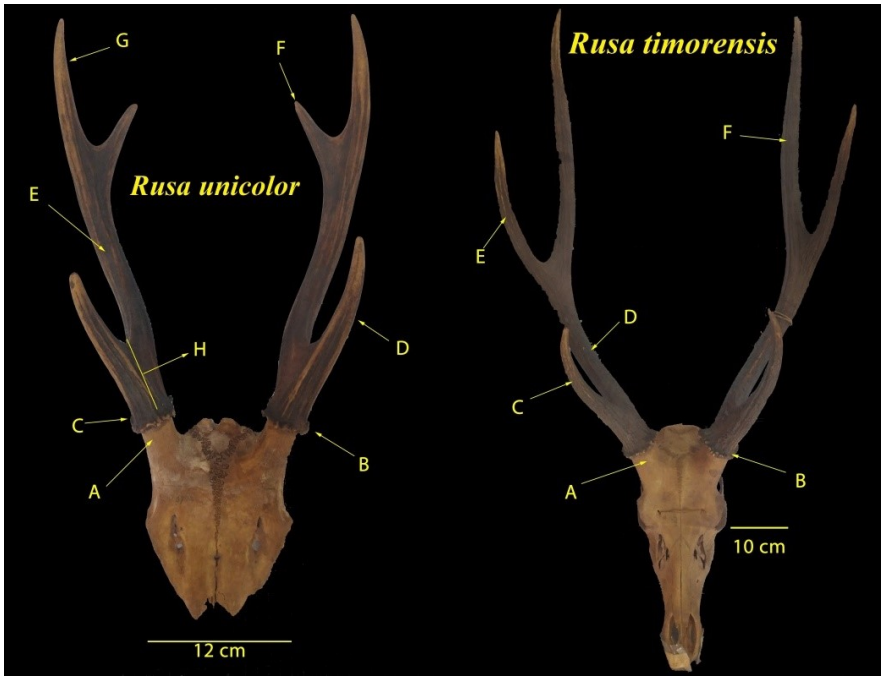

Figure 9. Specimens of *Rusa unicolor* (left) and *Rusa timorensis* (right), with description: A. Pedicle, B. Burr, C. Brow, D. 2nd segment of main beam, E. Bez, F. 3rd segment of main beam.

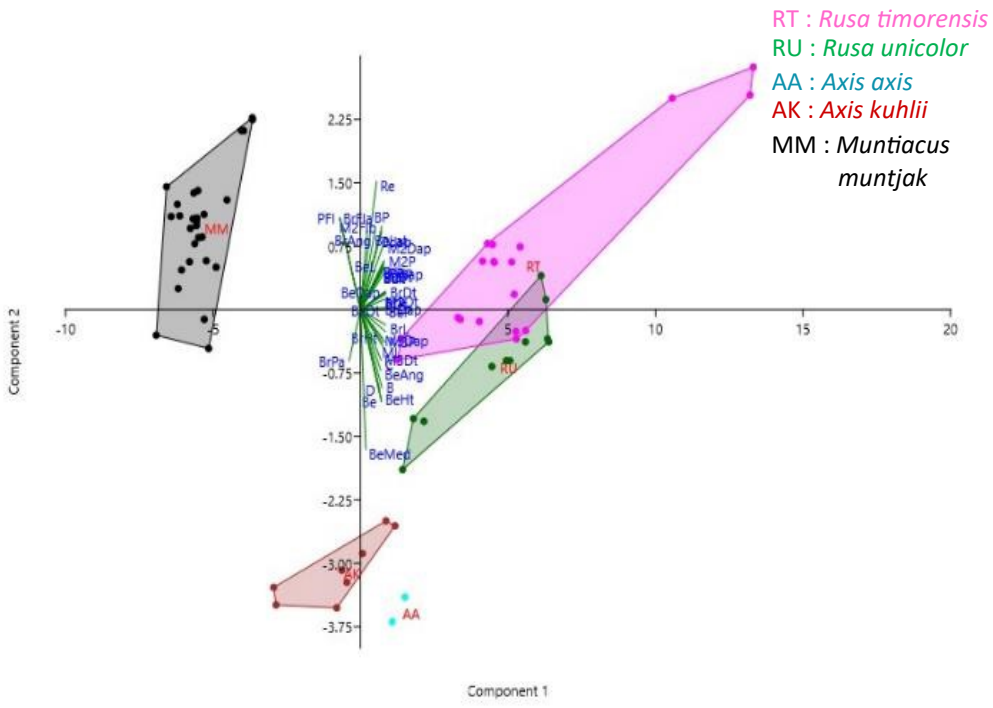

Figure 10. PCA result of paired antler specimens.

antler could experience abnormality or damage. The abnormality in antler's growth and damage can alter the shape and size of the antler. The branch which is not normally present in the antler is called "abnormal" or "accessory". Antlers growth can also be faster or slower in some individuals. The alteration of growth speed can also alter the maximum size of antlers. Therefore, some individuals of the species can have a different antler's characteristic from the one described in this article.

Diagnostic characters of antlers for each species

Based on the analysis, it can be seen that each group is separated from the others. That grouping is supported by some characters. The characters which

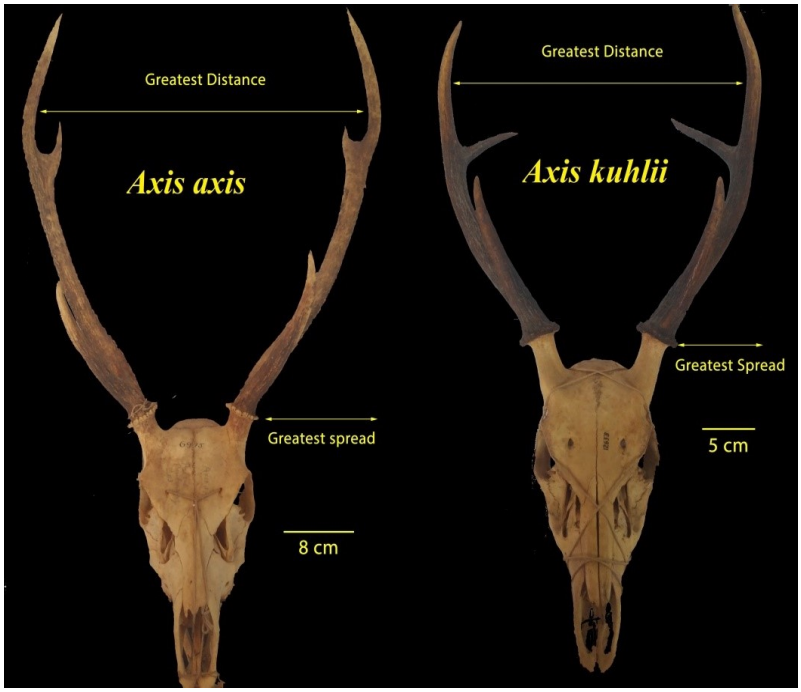

Figure 11. Comparison of antler's distance in *Axis axis* (left) and *Axis kuhlii* (right)

Table 4. Diagnostic characters of the antlers.

No	Species	Characters	Remarks
1	*Muntiacus muntjak*	Brow as the only branch	
		Pedicle long and flattened	
		Main beam flattened laterolaterally	Especially on the tip
		Brow flattened anteroposteriorly	Does not flattened on some individuals
		Low BrHt	0.7–2 cm
		Relief weak to strong	
2	*Axis axis*	Relatively widely curved	Not significant in some individuals, especially young ones
		BrHt intermediate	3–4 cm
		Brow angle intermediate	Approximately 50°
		Bez grows inward	
		Low *bez* angle	Around 35–40°, forms U-shape
		Weak relief	
3	*Axis kuhlii*	Relatively upright	
		BrHt intermediate	3–4 cm
		Brow angle intermediate	Approximately 50°
		Bez grows inward	
		Relatively high *bez* angle	Around 60–70°, forms L-shape
		Weak relief	
4	*Rusa unicolor*	Large diameter	Usually > 2cm
		Bez grows inward	
		Bez angle intermediate	Around 45–65°
		Brow angle intermediate	Around 40–55°
		High BrHt	Around 5–8 cm
		Extensions on branching	Especially on brow, forms area connecting brow and main beam
		Strong relief	Pearled in some individuals
5	*Rusa timorensis*	Large diameter	Usually > 2cm
		Bez grows outward	
		Bez angle intermediate	Around 50–70°
		Brow angle intermediate	Around 35–60°
		Extensions on branching	Especially on *bez*, forms area connecting *bez* and main beam
		Relief mostly pearled	No pearl but have strong relief in some individuals

supported a certain group become that group's diagnostic characters shown on Table 4.

CONCLUSION

Based on the research, it can be concluded that antler's characters could become diagnostic characters to identify cervids species. The diagnostic characters are pedicle, main beam, relief, brow, bez, and diameter of the antlers. *Muntiacus atherodes*'s and *Muntiacus montanus*'s antlers need to be analysed to distinguish it from *Muntiacus muntjak*.

REFERENCES

Bubenik, G.A. & Bubenik, A.B., 1990, *Horns, Pronghorns, and Antlers: Evolution, Morphology, Physiology, and Social Significance*, Springer-Verlag, New York, pp. 146–148.

Boone & Crockett Club. *Antler Measurements*, in Miller, K.V. & Marchinton, R.L., 1995, *Quality Whitetails*, Stackpole Books, Mechanicsburg, pp. 33–34.

CITES, 2003, *CITES Identification Guide – Hunting Trophies*, Ministry of Supply and Services Canada, pp. key 8–13, y 2–23.

Goss, R.J., 1985, *Deer Antlers: Regeneration, Function, and Evolution*, Academic Press, New York, pp. 1–2, 44–45.

Hedges, S., Duckworth, J.W., Timmins, R., Semiadi, G. & Dryden, G, 2015, *Rusa timorensis. The IUCN Red List of Threatened Species* 2015: e.T41789A22156866, viewed 2 September 2019. http://dx.doi.org/10.2305/IUCN.UK.2015-2.RLTS.T41789A22156866.en.

Heffelfinger, J., 2006, *Deer of the Southwest: A Complete Guide to the Natural History, Biology, and Management of Southwestern Mule Deer and White-Tailed Deer,* Texas A&M University Press, College Station, pp. 77–88.

McPherson, J. & McPherson, G., 2008, *Ultimate Guide to Wilderness Living*, Ulysses Press, Berkeley, pp. 57–59.

Ministry of Environment and Forestry, 2018, P.20/MENLHK/SETJEN/KUM.1/6/2018.

Price, J.S., Allen, S., Faucheux, C., Althnaian, T., & Mount, J.G., 2005, Deer Antlers: A Zoological Curiosity or the Key to Understanding Organ Regeneration in Mammals?, *Journal of Anatomy* 207, 603–618.

Prothero, D.R. & Foss, S.E., 2007. *The Evolution of Artiodactyls*, John Hopkins University Press, Baltimore, pp. 249–250.

Semiadi, G., Duckworth, J.W. & Timmins, R, 2015, *Axis kuhlii. The IUCN Red List of Threatened Species* 2015: e.T2447A73071875, viewed 2 September 2019. http://dx.doi.org/10.2305/IUCN.UK.2015-2.RLTS.T2447A73071875.en.

Semiadi, G., Subekti, K., Sutama, I. K., Masy'ud, B., & Affandy, L., 2003. Antler's Growth of the Endangered and Endemic Bawean Deer (*Axis kuhlii* Müller & Schlegel, 1842), *Treubia* 33(1), 89–95.

Stefoff, R., 2008, *Deer*, Marshall Cavendish, New York, pp. 47–55.

Timmins, R.J., Belden, G., Brodie, J., Ross, J., Wilting, A. & Duckworth, J.W, 2016a, *Muntiacus atherodes. The IUCN Red List of Threatened Species* 2016: e.T42189A22166396, viewed 2 September 2019. http://dx.doi.org/10.2305/IUCN.UK.2016-2.RLTS.T42189A22166396.en.

Timmins, R.J., Duckworth, J.W. & Groves, C.P., 2016b, *Muntiacus montanus. The IUCN Red List of Threatened Species* 2016: e.T136831A22168363, viewed 2 September 2019. http://dx.doi.org/10.2305/IUCN.UK.2016-1.RLTS.T136831A22168363_.en.

Walrod, D., 2010, *Antlers: A Guide to Collecting, Scoring, Mounting, and Carving*, Stackpole Books, Mechanicsburg, pp. 4–6, 83–85.

Journal of Tropical Biodiversity and Biotechnology
Volume 04, Issue 03 (2019): 107 — 112
DOI: 10.22146/jtbb.46256

Research Article

Genetic Identification of Freshwater Fish Species Through DNA Barcoding from Lake Lebo Taliwang, West Nusa Tenggara

Tuty Arisuryanti[1]*, Rika Lathif Hasan[1], Khadija Lung Ayu[1], Nofita Ratman[1], Lukman Hakim[1]

1) Laboratory of Genetics and Breeding, Faculty of Biology, Universitas Gadjah Mada, Jl. Tehnika Selatan Sekip Utara, Yogyakarta 55281, Indonesia

*Corresponding author, email address: tuty-arisuryanti@ugm.ac.id

Keywords:
genetic identification
freshwater fish
Lake Lebo Taliwang
DNA barcoding

Article history:
Submitted 27/05/2019
Revised 16/09/2019
Accepted 24/09/2019

ABSTRACT

Lake Lebo Taliwang is one of the lakes in the West Nusa Tenggara with high freshwater fish species diversity. However, the species identification of freshwater fish species from Lake Lebo Taliwang using DNA barcoding is very limited. Therefore, the objective of this study was to identify seven samples of freshwater fish species collected from Lake Lebo Taliwang based on *COI* mitochondrial gene as a DNA barcoding marker and establish library *COI* sequences of Indonesian freshwater fish. We are using a standard DNA analysis and data obtained from this study was then examined using Nucleotide BLAST and the phylogenetic tree was analyzed using the Neighbour-Joining (NJ) method with Kimura 2 Parameter (K2P) model. The results revealed that among the seven samples of freshwater fishes collected from the Lake Lebo Taliwang, three samples were identified as *Anabas testudineus*, the other three samples were *Barbodes binotatus* and one sample was *Trichopodus trichopterus*. The level of similarity of these freshwater fish samples referred to the database from the GenBank and BOLD was between 98 -100%. The NJ tree supports the clade of each species identified in this study. This occurrence indicated that DNA barcoding by using the *COI* mitochondrial gene was proven to be able to identify the freshwater fish samples accurately.

INTRODUCTION

Indonesia is an archipelago country with more than 17,000 islands and has high biodiversity including freshwater fish diversity, either living in the lakes, rivers, or swamps. Indonesia also has more than 840 lakes, and 17 of the lakes are located in the West Nusa Tenggara Province (NTB) (Haryani, 2013). One of the lakes located in West Nusa Tenggara is Lake Lebo Taliwang. Lake Lebo Taliwang is located in the two districts in the West Sumbawa Regency which are Taliwang District and Seteluk District. Taliwang District and Seteluk District are located around ± 15 m above sea level and ± 50 m above sea level, respectively. The water in Lake Lebo Taliwang comes from Suning River, Seran River, and flood overflow from Brang Rea River, with the total catchment area of 86 km² from West Seteluk direction. The total area of Lake Lebo Taliwang is 70% located in Taliwang District, and the rest 30% is located in Seteluk District. Many kinds of commercially freshwater fish inhabit in this area, such as grass carp, climbing perch, barb fish, swamp eel, and striped snakehead (RIPED, 2008). All of the freshwater fish inhabited at Lake Lebo Taliwang is commonly identify morphologically which is usually inaccurate and incorrect. This is due people identify the fish based on their morphology, which commonly similar between one and another, for example, between climbing perch and gourami (RIPED, 2008). Therefore, molecular identification using the *COI* gene as a DNA barcoding marker is needed to investigate the correct species name of the freshwater fish collected from Lake Lebo Taliwang. This is due to *COI* gene as a DNA barcoding marker has many advantages such as it can be used for small amount samples, all of the life stages, and differentiation between similar phenotypes of fish (Dudu *et al.*, 2016).

The application of DNA barcoding in the form of sequence data of cytochrome c oxidase subunit I mitochondrial gene (mtDNA-*COI*) has been extensively used for taxonomy study and

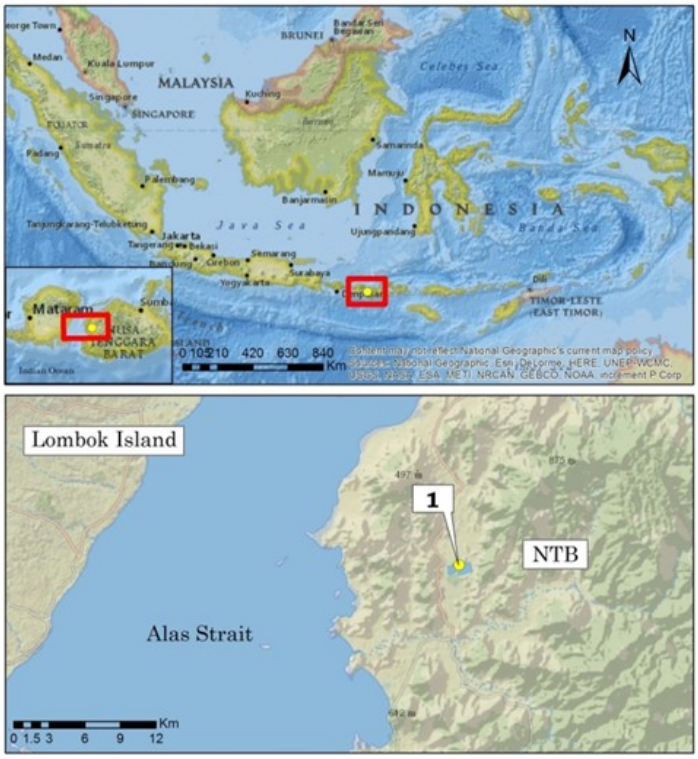

Figure 1. Map of sampling collection sites for freshwater fish samples in Lake Lebo Taliwang,

organism identification (Hebert *et al*., 2003; Arif and Khan, 2009; Chauhan and Rajiv, 2010; Yudhistira and Arisuryanti, 2019). Besides, it has been useful for the identification of genetically divergent wild stocks of conservation significance for a number of fish species such as mudskipper (Arisuryanti *et al*., 2018), marine eels (Peninal *et al*., 2017), and Asian red catfish (Syaifudin *et al*., 2017). It is now considered highly desirable to include sequences from mitochondrial *COI* gene to identify freshwater fish species accurately (Dahruddin *et al*., 2017; Hutama *et al*., 2017). This is due to proper species database information can be implemented for conservation and breeding program. Therefore, the objective of this study was to identify freshwater fish species collected from Lake Lebo Taliwang using *COI* mitochondrial gene as a DNA barcoding marker and establish *COI* sequence library of freshwater fish in Indonesia, especially from Lake Lebo Taliwang, West Nusa Tenggara.

MATERIALS AND METHODS

Sample Collection, DNA extraction, amplification, and sequencing

Twenty freshwater fish samples were collected from Lake Lebo Taliwang, West Nusa Tenggara (Figure 1) either from fisherman or by hand net. From the twenty samples which were caught in the field, we grouped three fish group based on their similar phenotypes and chose seven samples as a representative of the three group fish samples. Then, a cube of lateral muscle (6-8 mm) from the left side of the fish was exercised for DNA extraction. The muscle tissue was put into a 1.5 ml sterile tube and preserved in 99% ethanol. All samples were then brought to the Laboratory of Genetics and Breeding, Faculty of Biology, Universitas Gadjah Mada (Yogyakarta, Indonesia) and were kept in -20^{o}C for further analysis.

DNA genomic from muscle tissue of each sample was extracted using DNeasy Blood and Tissue Kit (Qiagen, USA) according to the supplier's protocol. COI mitochondrial gene of each sample was then amplified by polymerase chain reaction (PCR) using the universal primers FishF2 (5'-TCGACTAATCATAAAGATATCGGCAC-3') and FishR2 (5'-ACTTCAGGGTGACCGAAGAATCA GAA-3') designed by Ward *et al.* (2005). Each 25 µl reaction contained 3 µl (10-100 ng) DNA template, 12.5 µl of MyTaq HS Red Mix PCR kit (Bioline), 2 µl of 2 mM $MgCl_2$, 1.5 µl of 0.6 µM of each primer and 5.5 µl double distilled water (ddH_2O). A negative control has to be included for evaluating the reliability of the DNA amplification by omitting template DNA from the reaction mixture. PCR amplification conditions were 2 min pre-denaturation at 95^{o}C, followed by 35 cycles of denaturation at 95^{o}C for 15 sec, annealing at 50^{o}C for 30 sec, and extension at 72^{o}C for 30 sec. A final extension of 5 min at 72^{o}C was performed. We examined the PCR products on 1% agarose gels,

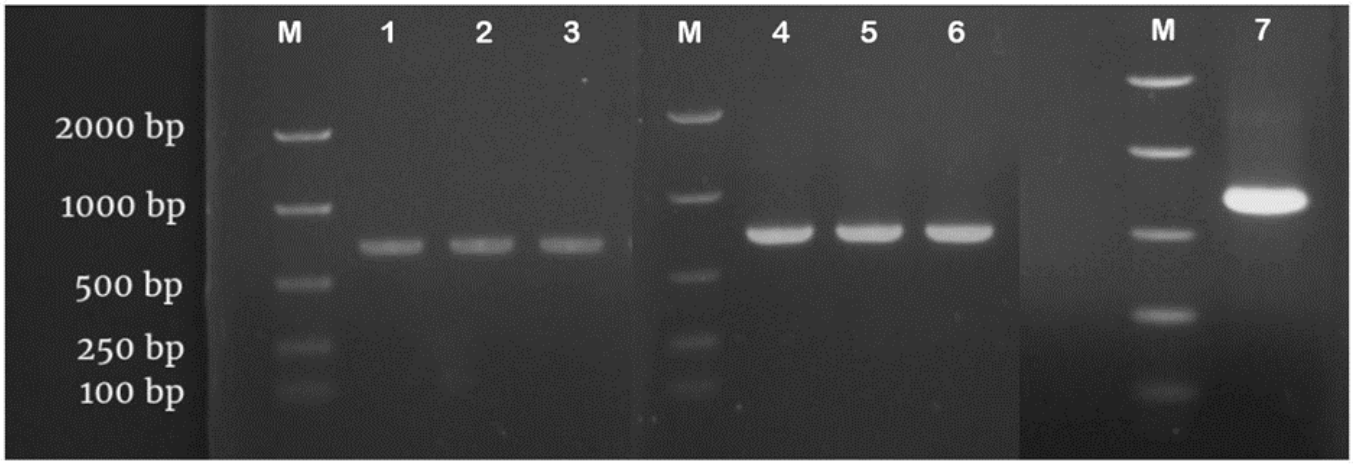

Figure 2. DNA profiles resulted from PCR amplification of *COI* mitochondrial genes of seven fish samples collected from Lake Lebo Taliwang, West Nusa Tenggara. (M=marker)

purified with ExoSAP-IT™PCR purification kit (Applied Biosystems) and sequenced with the automated sequenced using the dye-termination method (Big Dye Terminator Ver. 3.1., Applied Biosystems), 20-50 ng purified PCR product, and 0.8 µM of either primer per reaction. The amplicons were sequenced in both forward and reverse directions. Fragments were then analyzed on an ABI 3500 Genetic Analyzer (Applied Biosystems) automated sequencer. DNA genomic from muscle tissue of each sample was extracted using DNeasy Blood and Tissue Kit (Qiagen, USA) according to the supplier's protocol. COI mitochondrial gene of each sample was then amplified by polymerase chain reaction (PCR) using the universal primers FishF2 (5'-TCGACTAATCATAAAGATATCGGCAC-3') and FishR2 (5'-ACTTCAGGGTGACCGAAGAAT CAGAA-3') designed by Ward *et al.* (2005). Each 25 µl reaction contained 3 µl (10-100 ng) DNA template, 12.5 µl of MyTaq HS Red Mix PCR kit (Bioline), 2 µl of 2 mM $MgCl_2$, 1.5 µl of 0.6 µM of each primer and 5.5 µl double distilled water (ddH_2O). A negative control has to be included for evaluating the reliability of the DNA amplification by omitting template DNA from the reaction mixture. PCR amplification conditions were 2 min pre-denaturation at 95°C, followed by 35 cycles of denaturation at 95°C for 15 sec, annealing at 50°C for 30 sec, and extension at 72°C for 30 sec. A final extension of 5 min at 72°C was performed. We examined the PCR products on 1% agarose gels, purified with ExoSAP-IT™PCR purification kit (Applied Biosystems) and sequenced with the automated sequenced using the dye-termination method (Big Dye Terminator Ver. 3.1., Applied Biosystems), 20-50 ng purified PCR product, and 0.8 µM of either primer per reaction. The amplicons were sequenced in both forward and reverse directions. Fragments were then analyzed on an ABI 3500 Genetic Analyzer (Applied Biosystems) automated sequencer.

Data Analyses

Forward and reverse sequences were edited and used to build consensus sequences with SeqMan and EditSeq (Lasergene, DNASTAR). The mitochondrial *COI* sequence of each specimen was converted into FASTA format and analysed using nucleotide BLAST (blast.ncbi.nlm.gov) and BOLD databases for species identity confirmation (www.boldsystems.org) (Ratnasingham and Hebert, 2007). The sequences were then aligned using opal multiple sequence alignment in MESQUITE v.3.51 (Madison & Madison, 2018) and ClustalW in MEGA7 (Kumar *et al.*, 2016). Next, sequences were compared by the Neighbour-Joining (NJ) method by applying the correction of the model Kimura 2-parameter (K2P). The analysis of confidence estimates of the relations in the NJ trees was performed with a bootstrap analysis of 1000 replications with the program MEGA7 (Tamura *et al.*, 2016). The NJ tree-based method was followed for the identification of unidentified specimens. This method assumed that query sequences belonged to a specific species if they were incorporated within a cluster (Pettengil and Maile, 2010). The barcode sequences of five fishes were taken from GenBank and BOLD for identifying species and as a comparative purpose, and the *COI* sequence of *Penaeus monodon* was extracted from GenBank for an outgroup.

RESULT AND DISCUSSION

The research result indicated that the seven samples of freshwater fishes can be well amplified (Figure 2). All of the *COI* sequences from seven fish samples revealed no insertion, deletions and stop codons. The PCR products of the seven samples have

Table 1. Species identification based on GenBank database using BLAST analysis and BOLD identification

No	Sample Code	Identified species from GenBank/BOLD	Querry Cover (%)	Similarity (%)
1	Sample-1	*Barbodes binotatus* (MG699681)	95	100
2	Sample-2	*Barbodes binotatus* (MG699681)	95	100
3	Sample-3	*Barbodes binotatus* (MG699667)	96	99.84
4	Sample-4	*Anabas testudineus* (KU692243)	100	99.81
5	Sample-5	*Anabas testudineus* (KU692243)	100	99.81
6	Sample-6	*Anabas testudineus* (KU692243)	100	99.81
7	Sample-7	*Tricogaster trichopterus* (synonym: *Trichopodus trichopterus*)* (KC789556)	97	99.57
		Trichopodus trichopterus (KU569063)	92	100

*Source: Fricke *et al.* (2019)
Parentheses in each species related to the accession number in the GenBank

fragment lengths as follow: sample 1 was 666 bp (222 amino acid), sample 2 was 651 (217 amino acid), sample 3 was 636 bp (212 amino acid), sample 4 was 666 bp (222 amino acid), sample 5 was 703 (235 amino acid), sample 6 was 575 (179 amino acid), and sample 7 was 708 bp (236 amino acid). All of the *COI* sequences were submitted and published in the GenBank with the following accession numbers: samples 1-3 (MN640073-MN640075), samples 4-6 (MN640070-MN640072), and sample 7 (MN623381).

The nucleotide BLAST analysis result and identification through BOLD showed that the seven data of COI mitochondrial gene sequence of the fishes from the Lake Lebo Taliwang can could be grouped into three species (Table 1). The sequences of *COI* mitochondrial gene of sample 1, 2 and 3 have similarity 99.8-100% if compared to *Barbodes binotatus* recorded in the GenBank database by applying BLAST analysis and BOLD identification. Therefore, the fish sample number 1, 2 and 3 were verified as *Barbodes binotatus*. Further, the sequence of *COI* mitochondrial gene of sample 4, 5, and 6 have similarity 99.84-100% if compared to *Anabas testudineus* as in the GenBank database by using BLAST analysis and through BOLD identification. It means the three fish samples (sample number 4, 5, and 6) were confirmed as *Anabas testudineus*. Next, the sequence of the *COI* mitochondrial gene of sample 7 has similarity 99.57-100% compared to *Trichopodus trichopterus* in the GenBank database through BLAST analysis and BOLD identification. Based on this analysis, the sample number 7 was verified as *Trichopodus trichopterus*. According to Yang *et al.* (2014), if the specimen has the similarity score between 98-100% with the species which has been recorded at the GenBank or BOLD, the specimen can be named as the identified species recorded at the GenBank or BOLD with that high score similarity.

The grouping of the three species was supported by the Neighbour Joining (NJ) tree (Figure 3). From Figure 3, it can be seen that sample 1, 2 and 3 was clustered with *Barbodes binotatus* (accession number MG699667 and MG699681). Next, sample 4, 5 and 6 were clustered with *Anabas testudineus* (accession number KU692243) whereas sample 7 was clustered with *Tricogaster trichopterus* (accession number KC789556) and *Trichopodus trichopterus* (KU569063). According to Fricke *et al.* (2019), *Tricogaster trichopterus* is synonym with *Trichopodus trichopterus*.

The result of genetic identification by using *COI* mitochondrial gene as DNA barcoding had been able to detect seven samples collected from Lake Lebo Taliwang, West Nusa Tenggara and were classified into three species. It indicates that the sequence of the *COI* mitochondrial gene as a DNA barcoding marker can be used to identify the fish samples more accurately and quickly. In addition, the *COI* sequences from the three fish species can be implemented as the *COI* library sequences which are useful to identify the life cycle of the three species (egg, larvae, juvenile and adult).

CONCLUSION

The sequence of *COI* mitochondrial gene as a DNA barcoding marker was able to identify the seven samples of fishes from Lake Lebo Taliwang, West Nusa Tenggara, which were classified into three species, three samples were *Barbodes binotatus*, the other three samples were *Anabas testudineus,* and one sample was *Trichopodus trichopterus*. The *COI* sequences from the three fish species can be implemented as the *COI* library sequences.

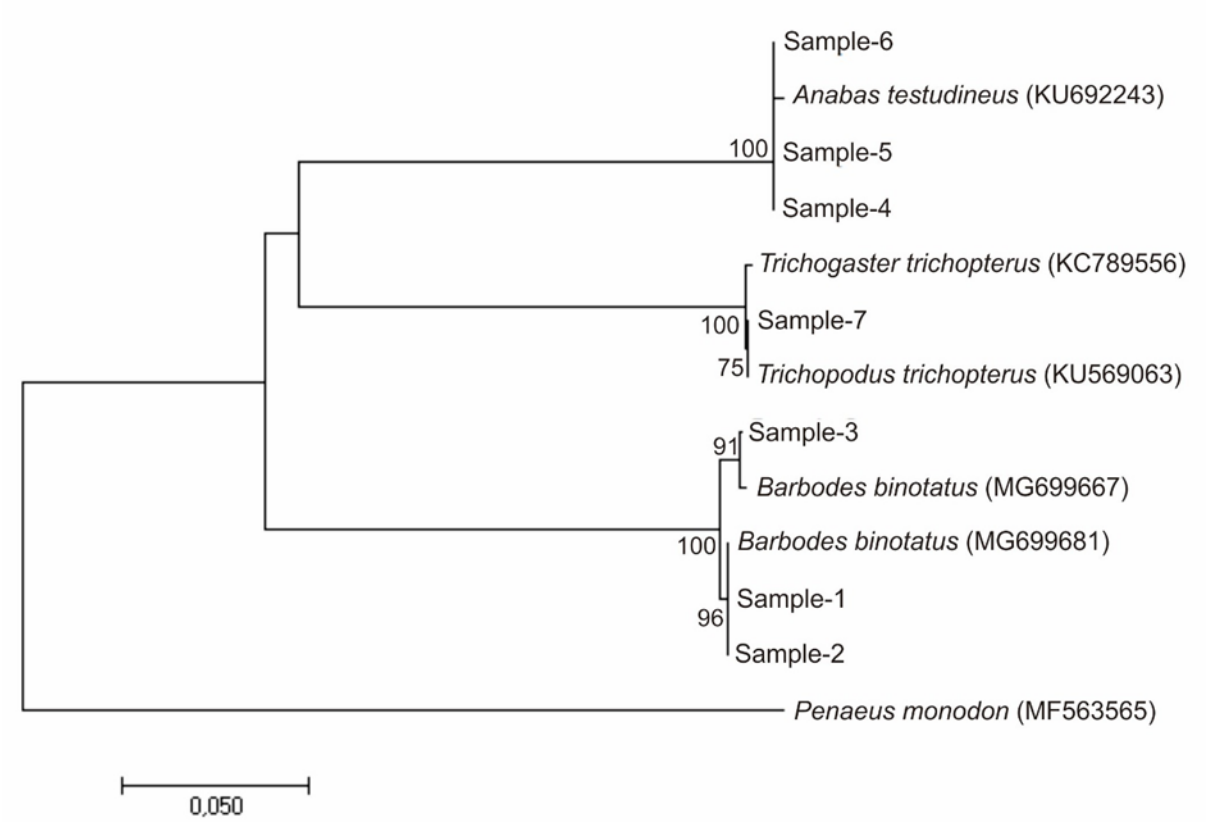

Figure 3. Neighbour-joining tree based on COI sequence data using the Kimura two-parameter (K2P) substitution model. The number at each node represents bootstrap and scale corresponds to substitution/site.

ACKNOWLEDGEMENT

The author sincerely appreciates the support from the Head of the Laboratory of Genetics and Breeding, Faculty of Biology UGM, and the Head of Integrated Research and Testing Laboratory (LPPT) UGM, who have provided facilities and tools for this research.

REFERENCES

Arif, I.A. & Khan, H.A., 2009, Molecular markers for biodiversity analysis of wild animals: a brief review, Animal Biodiversity and Conservation, 32(1), 9-17.

Arisuryanti, T., Hasan, R.L. & Koentjana, J.P., 2018, Genetic identification of two mudskipper species (Pisces: Gobiidae) from Bogowonto Lagoon (Yogyakarta, Indonesia) using *COI* mitochondrial gene as a DNA barcoding marker, *AIP Conference Proceedings*, 2002, 020068 (1)-020068(7).

Chauhan, T. & Rajiv, K., 2010, Molecular markers and their applications in fisheries and aquaculture, *Advances in Bioscience and Biotechnology*, 01(04), 281-291.

Dahruddin, H., Hutama, A., Busson, F., Sauri, S., Hanner, R., Keith, P., Hadiaty, R., & Hubert, N., 2017, Revisiting the ichthyodiversity of Java and Bali through DNA barcodes: taxonomic coverage, identification accuracy, cryptic diversity and identification of exotic species, *Molecular Ecology Resources*, 17(2), 288-299.

Dudu, A., Barbălată, T., Popa, G., Georgescu, S.E., Costache, M., 2016, Advantages and limitations of DNA Barcoding in identifying commercially-exploited fish species, *Animal Science and Biotechnologies*, 49 (1), 45-49.

Fricke, R., Eschmeyer, W. N. & Van der Laan, R., 2019, Eschmeyer's catalog of fishes: genera, species, references, viewed 1 June 2019, http://researcharchive.calacademy.org/research/ichthyology/catalog/fishcatmain.asp.

Haryani, G., 2013, Kondisi danau di Indonesia dan strategi pengselolaannya. *Prosiding Pertemuan Ilmiah Tahunan Masyarakat Limnologi Indonesia* I, 1-19.

Hebert, P.D., Ratnasingham, S. & deWaard, J.R., 2003, Barcoding animal life: cytochrome c oxidase subunit 1 divergence among closely related species, *Proceedings of the Royal Society B: Biological Sciences*, 270 Suppl 1, S96-99.

Hutama, A., Dahruddin, H., Busson, F., Sauri, S., Keith, P., Hadiaty, R.K., Hanner, R., Suryobroto, B. & Hubert, N., 2017, Identifying spatial concordant evolutionary significant units across multiple species through DNA barcodes: Application to the conservation genetics of the freshwater fishes of Java and Bali, *Global Ecology and Conservation*, 12, 170-187.

Kumar, S., Stecher, G., & Tamura, K., 2016, MEGA7: molecular evolutionary genetic analysis version 7.0 for bigger datasets, *Molecular Biology and Evolution*, 33(7), 1870-1874.

Librado, P., & Rozas, J., 2009, DnaSP v5: a software for comprehensive analysis of DNA polymorphism data. *Bioinformatics*, 25(11), 1451 -1452.

Maddison, W.P., & Maddison, D.R., 2018, Mesquite: A modular system for evolutionary analysis. Version 3.51 http://www.mesquiteproject.org.

Peninal, S., Subramanian, J., Elavarasi, A. & Kalaiselvam, M., 2017, Genetic identification of marine eels through DNA barcoding from Parangipettai coastal waters. *Genomics Data*, 11, 81-84.

Pettengill, J.B. & Maile, C.N., 2010, An evaluation of candidate plant DNA barcodes and assignment methods in diagnosing 29 species in the genus *Agalinis* (Orobanchaceae). *American Journal of Botany,* 97,1391–1406.

Ratnasingham, S. & Hebert, P.D.N., 2007, BOLD: The barcode of life data system (www.barcodinglife.org). *Molecular Ecology Notes*, 7, 355-364.

RIPED, 2008, Lebo Taliwang, kekayaan flora dan fauna Sumbawa Barat, viewed 27 February 2019, http://konservasi4lebotaliwang.blogspot.com

Syaifudin, M., Jubaedah, D., Muslim, M. & Daryani, A., 2017, DNA authentication of Asian Red Catfish *Hemibragus nemurus* from Musi and Penukal River, South Sumatra Indonesia. *Genetics of Aquatic Organisms*, 1, 43-48.

Yang, L., Tan, Z.,Wang, D., Xue, L., Guan, M-X., Huang, T. & Li, R., 2014, Species identification through Mitochondrial rRNA genetic analysis. *Scientific Reports*, 4:4089.

Yudhistira, A & Arisuryanti, T., 2019, Preliminary findings of cryptic diversity of the giant tiger shrimp (*Penaeus monodon* Fabricius, 1798) in Indonesia inferred from *COI* mitochondrial DNA. *Genetika,* 51, 261-270.

Ward, R.D., Zemlak, T.S., Innes, B.H., Last, P.R., & Hebert, P.D.N., 2005, DNA barcoding Australia's fish species. *Philosophical Transactions of the Royal Society B*, 360(1462), 1847-1857.

Journal of Tropical Biodiversity and Biotechnology
Volume 04, Issue 03 (2019): 113 — 118
DOI: 10.22146/jtbb.39275

Research Article

The Effect of Ethanolic Extract of Cashew Fruit Peel on The Liver Histological Structure in Rat (*Rattus norvegicus* Berkenhout, 1769)

Laili Mufli Zusrina[1], Nastiti Wijayanti[1], and Bambang Retnoaji[1]*
1) Faculty of Biology, Universitas Gadjah Mada, Jl. Teknika Selatan, Sekip Utara, Yogyakarta, 55128
*Corresponding author, tel.: +6281325722515, email address: bambang.retnoaji@ugm.ac.id

Keywords:
cashew fruit
peel
extract
mouse
liver
histology

Article history:
Submitted 01/10/2018
Revised 03/09/2019
Accepted 21/09/2019

ABSTRACT
Cashew fruit peel is a waste produced from the cashew nut industry, and it has not been utilized optimally yet. Cashew peel extract has the potential to be used as a contraceptive agent, which capable of reducing reproductive capacity. However, its side effects on other tissue and organ such as liver not clearly studied yet. This study aims to determine the effect of ethanolic extracts of cashew peel on the histological structure of the white rat liver. In this study, 21 female white rats were used and be grouped for control (6 mice) which were treated with CMCMa 0.5% and 15 mice were treated with peel extract of 500 mg/kg body every day for one month. Liver for examination was collected sequentially at 3rd, 5th, 8th, 11th, and 14th of the estrous cycle. The liver was processed for histological observation and stained with Hematoxylin Eosin and Mallory Acid Fuchsin staining solution. The liver hepatocyte was observed for it abnormality and be scored to calculate the number of cell damage or abnormality. The result showed that peel extract-treated mouse liver was similar to control ones; we did not witness any evidence of fibrosis, pyknosis and cellular necrosis on either control or treated mouse. Statistical analysis by SPSS showed that the p-value between the control and treatment groups was 0.078 (> 0.05) so there was no significant difference between control and treatment. It could be concluded that ethanolic extracts of cashew nuts peel with a concentration of 500 mg/kg body weight caused no effect on the mouse liver histological structure. application with reduced-dosages of NPK fertilizers were arranged in a random block design with three replicates. The results show that large quantities of silica bodies attached to the surface of EFB fibers and amounting to 0.44% soluble Si. The FFB data indicated that the application of 75% NPK + 500 kg composted EFB + 2 L BioSilAc/ha/year on a five-year-old plant resulted in higher yield than that obtained from 100% standard dosage of NPK. The study also revealed that the application of EFB compost reduced 50% of BioSilAc dosage.

INTRODUCTION
The potential of cashew cultivation in Indonesia is promising, especially in the eastern part of Indonesia. Production of cashew from year to year has increased, as in 1999, nuts cashew production reached to 88,658 tons, and increased to 94,439 tons in 2002 (BPS, 2002). Cashew fruit peel is a waste produced from the cashew nut industry, and it has not been utilized optimally yet. Cashew nut fruit peel (shell) contain oil known as Cashew Nut Shell Liquid (CNSL). The main components of CNSL are anacardate acid, cardanol and cardol (Patel, 2016).

According to Harlita (2016), cashew peel extract has an antifertility effect by changing the uterine structure of albino rats. In addition, Herlina's (2013) also shown that cashew fruit extracts (*Anacardium occidentale* L.) had cytotoxic and estrogenic activity, decreased body weight and also testosterone levels on white mice.

The liver is the main organ that responsible for detoxification of hazard or harmful compounds that enter the body and also protecting the body against the accumulation of harmful substances from outside and inside. The liver also the site where

drugs and other toxic substances are metabolised (Sativani, 2010). The presence of hazard compounds inside the body could cause an adverse effect on the histological structure and physiological function of the liver. Research on the effect of ethanolic extracts of cashew (*Anacardium occidentale*) peel on liver organ histopathology has never been done, therefore this study is important to know the effect of giving ethanolic extract of cashew (*Anacardium occidentale*) peel on the histological structure of the liver in Wistar mouse as a model animal (*Rattus norvegicus* Berkenhout, 1769).

MATERIALS AND METHODS

Materials

This research was conducted from February to July 2018 at the Laboratorium Penelitian dan Pengujian Terpadu (LPPT) UGM and at the Histology Laboratory Faculty of Biology, Universitas Gadjah Mada. The material used in this study was cashew nut (*Anacardium occidentale* L.) which was dried and then extracted using ethanol 96% distillate, white rat (*Rattus norvegicus* Berkenhout 1769) 21-month old female Wistar strain, picric acid, Sodium solution Carboxyl Methyl Cellulose (CMCNa) 0.5%, ketamine, and physiological saline solution. The material for histology preparations was distilled water, Bouin solution, ethanol, toluene, 0.1% Acid Fuchsin solution, PMA solution, Mallory solution, paraffin, xylene, Meyer` s albumin, Ehrlich's hematoxylin, and Eosin-Y 1-2%.

Methods

Cashew nut seed extraction

Cashew seed peel was washed and dried in an oven at 30ºC for 72 hours and then ground to powder. The powder was soaked in 96% ethanol solution, stirred for 30 minutes, allowed to stand for 24 hours, and filtered. This step was repeated three times. The extract solution was separated and distilled at 70 ºC, and the oil was separated from the solvent using a vacuum rotary evaporator and a water bath heater. The thick extract was heated with a water bath while stirring it.

Treatment

Twenty one female white rats were divided into two groups: 6 mice as control and 15 mice for extract treatment, respectively. The control group were divided into two, which were untreated control and placebo control mouse, which were fed with 0.5% CMCNa. The treated group were fed with 500 mg extract/kg BW. Termination of the treatment was carried out during the 3rd (K3) , 5th (K4), 8th (K5), 11th (K6) and 14th (K7) estrous cycles. The mouse liver organs were collected and processed for histological preparation.

Treatment termination and organ collection

Mouse were euthanized with an overdose of ketamine, dissected, and the liver organ was taken and then was with a salt buffer for debris cleaning and post-mortem reaction delay.

Histology preparation for liver organ

The liver organs were collected, washed with salt buffer, fixed with Bouin's solution for 12 hours, and processed following paraffin standard method. The histological slides were stained with Haematoxylin-eosin and Mallory Acid Fuchsin staining.

Qualitative data were acquired from the descriptive analysis of treatment and control groups liver histological structure, using a microscope with a magnification of 10x10 and 10x100, respectively. Moreover, quantitative data was obtained from the number of defect cells, based on three layout view, which was analyzed with One Way ANOVA for social sciences (SPSS).

RESULTS AND DISCUSSION

Microscopic observation on Hematoxylin-Eosin stained liver showed that hepatocytes were in radial arrangement, with rounded-purple stained of nuclear cell positioned on the center of the cells. Sinusoid was radially arranged, which extends from the sinus area to the central vein at the center of the liver lobule. The extract-treated group of K3, K5, and K6 showed the sign of hepatocyte defect or degeneration, which were characterized by the occurrence of cytoplasmic vacuolization. It was also observed the appearance of some pyknotic cells, which were characterized by denser nuclear cell and the darker image of cell cytoplasmic content compared to control or normal cells (Figure 1). The pyknotic cells are one of the symptoms of the occurrence of cell damage. The nucleus of a pyknotic cell is smaller because of the irreversible chromatin and nucleus condensation, which is called the pyknosis process. Pyknosis usually occur in cells that experience apoptosis or necrosis (Hou et al., 2016).

The result showed that the percentage of the pyknotic cell on the control and placebo control group was 6% and 5.47%, respectively. Meanwhile, extract-treated mouse showed a relatively higher percentage of pyknotic cells, which the highest percentage of the pyknotic cell occurs at the group of K3 mouse of 8.93% (Figure 2).

Based on statistical analysis, the extract does not affect the percentage of rat liver cell damage

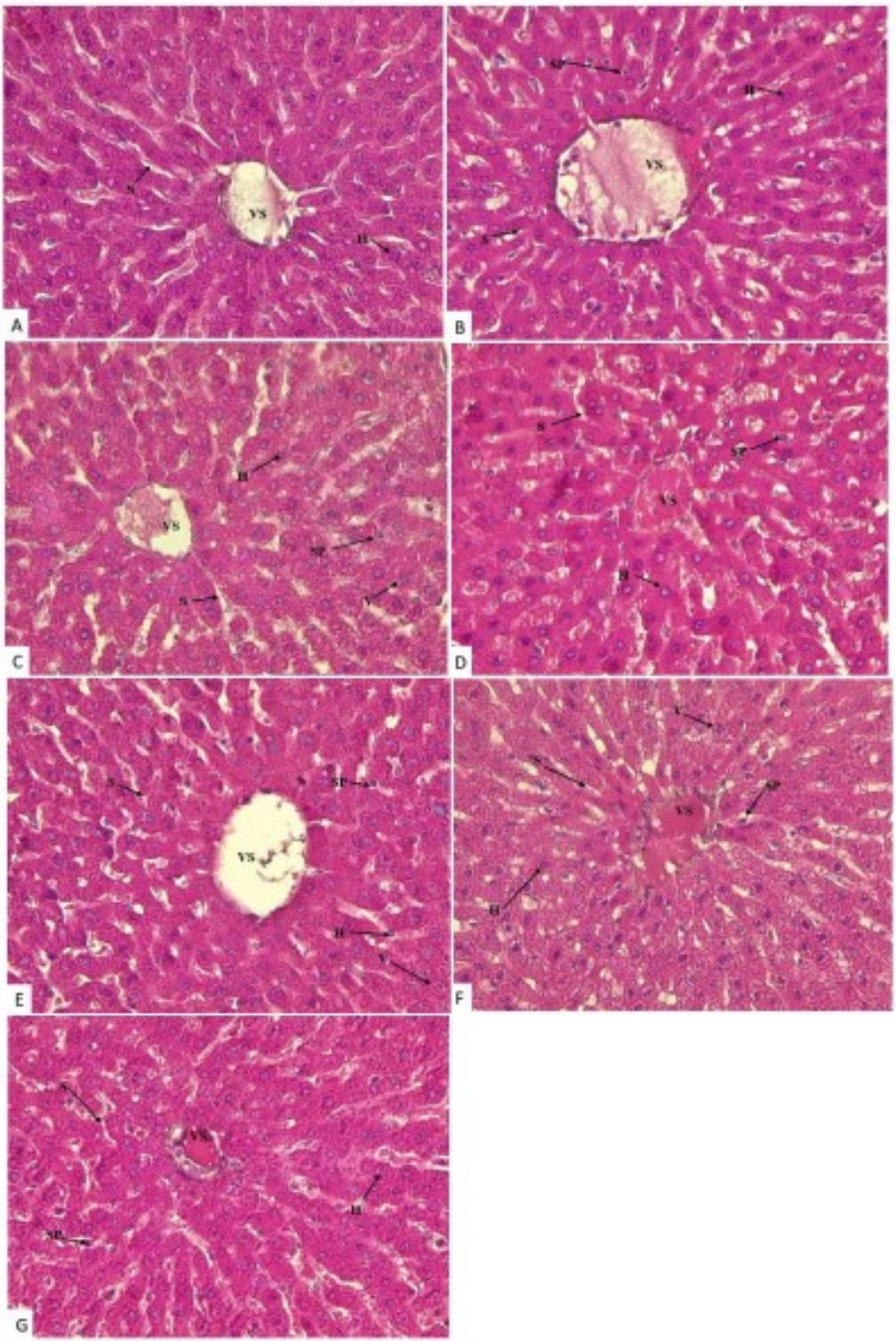

Figure 1. Histological structure of mouse liver group of A). control, B). placebo control, C). K3, D). K4, E). K5, F). K6 and G). K7. Central veins (VS), hepatocytes (H), pyknotic cells (SP), and sinusoids (S). K1= Control; K2= Placebo control; K3= termination at 3rd estrous cycle; K4= Termination at 5th estrous cycle; K5= termination at 8th estrous cycle; K6= termination at 11th estrous cycle; K7=termination at 14th estrous cycle. HE stained, 10x40 magnification.

significantly compared to control (P=0,05). Cell vacuolization was observed in several groups of the extract-treated mouse of K3, K5, and K6. Cell vacuolization is one of the characteristics of cell degeneration. The cells degeneration usually occurs as a response to cell injury or stress, which is reversible. If the toxic exposure is removed from the mouse, therefore the cells could be restored to normal and could resume its normal physiological condition. Cell degeneration is characterised microscopically by the presence of cell vacuolization, which is found in clear spaces in the cell cytoplasm (Carlton and McGavine, 1995). This condition is caused by metabolic disorders in the liver organ. Damage to the cell membrane causes leakage of the membrane which disrupts the activity of the K + transport that comes out of the cell, and the entry of Ca2 +, Na +, and water into the cell. Excessive

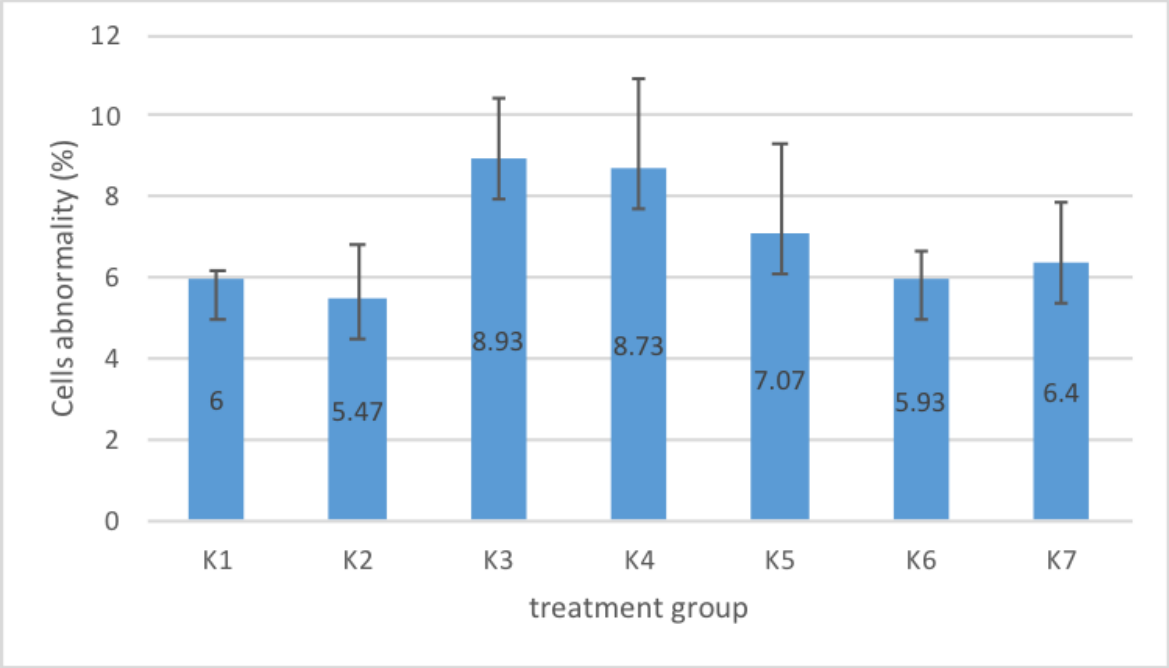

Figure 2. Percentage of pyknotic cells on the liver of control and extract treated mouse. K1= Control; K2= Placebo control; K3= termination at 3rd estrous cycle; K4= Termination at 5th estrous cycle; K5= termination at 8th estrous cycle; K6= termination at 11th estrous cycle; K7=termination at 14th estrous cycle

extracellular fluid influx causes cytoplasmic inflating, mitochondria, and coarse endoplasmic reticulum (King and Joseph, 1996).

The liver is the main organ that functions as detoxification of harmful substances in the body. The detoxification of harmful substances in the liver consists of phase I and phase II processes. Generally harmful substances that are not needed by the body, are easily soluble in lipids (lipophilic) naturally and difficult to pass through the cell membrane in the process of excretion. The liver is able to change the chemical components of harmful substances through several reactions such as oxidation and conjugation. This reaction will produce compounds that are more polar and water-soluble so that easily to be excreted through urine or bile. In phase I detoxification there is an oxidation reaction involving the cytochrome P450 enzyme. Whereas, phase II detoxification, is a conjugation reaction where small polar molecules are added to the chemical substance so that the substance is water-soluble (Chiang, 2014).

Microscopic observation of the liver was also carried out with Mallory-Acid Fuchsin staining to observe the presence of fibrosis in the liver connective tissue. Liver fibrosis usually occurs in the form of accumulation of extracellular matrix in response to various stimuli and causes various liver function disorders and blood flow. When fibrosis occurs in the tissue, normal tissue will be replaced by non-functional connective tissue which can further reduce the physiological function of the liver. Fibrosis is divided into several scales, consisting of F0, F1, F2, F3, and F4. F0 is the smallest scale where fibrosis is not found, or there is no enlarged portal tract and septa. F1 is characterized by portal fibrosis without septa. F2 is characterized by portal fibrosis with little septa or fibrous tissue around the portal tract. The F3 scale is indicated by the presence of portal fibrosis with many septa or fibrous tissue that connects the portal tract with the portal tract or with a central vein or bridging fibrosis, and the F4 scale is characterized by cirrhosis (Bedossa, 1994).

Observations result on liver tissue, which stained with Mallory-Acid Fuchsin, showed the presence of connective tissue in the form of collagen, be shown in blue color (Figure 3). The collagen fiber can be found at the area around the central vein, and there was no difference in collagen composition of both control and treatment groups. Moreover, It was also evidenced by the absence of fibrosis symptoms in the portals vein, nor the formation of septa between one lobe and the other (Figure 3). The observation results leading to the conclusion that the extract does not affect the connective tissue damage in the histological structure of mouse liver.

CONCLUSIONS

It can be concluded that ethanolic extracts of cashew peel did not affect the histological structure of liver of mouse (*Rattus norvegicus* Berkenhout, 1769), which was characterized by no significantly different between the control and treatment group on cell damage and fibrotic liver tissue of the mouse.

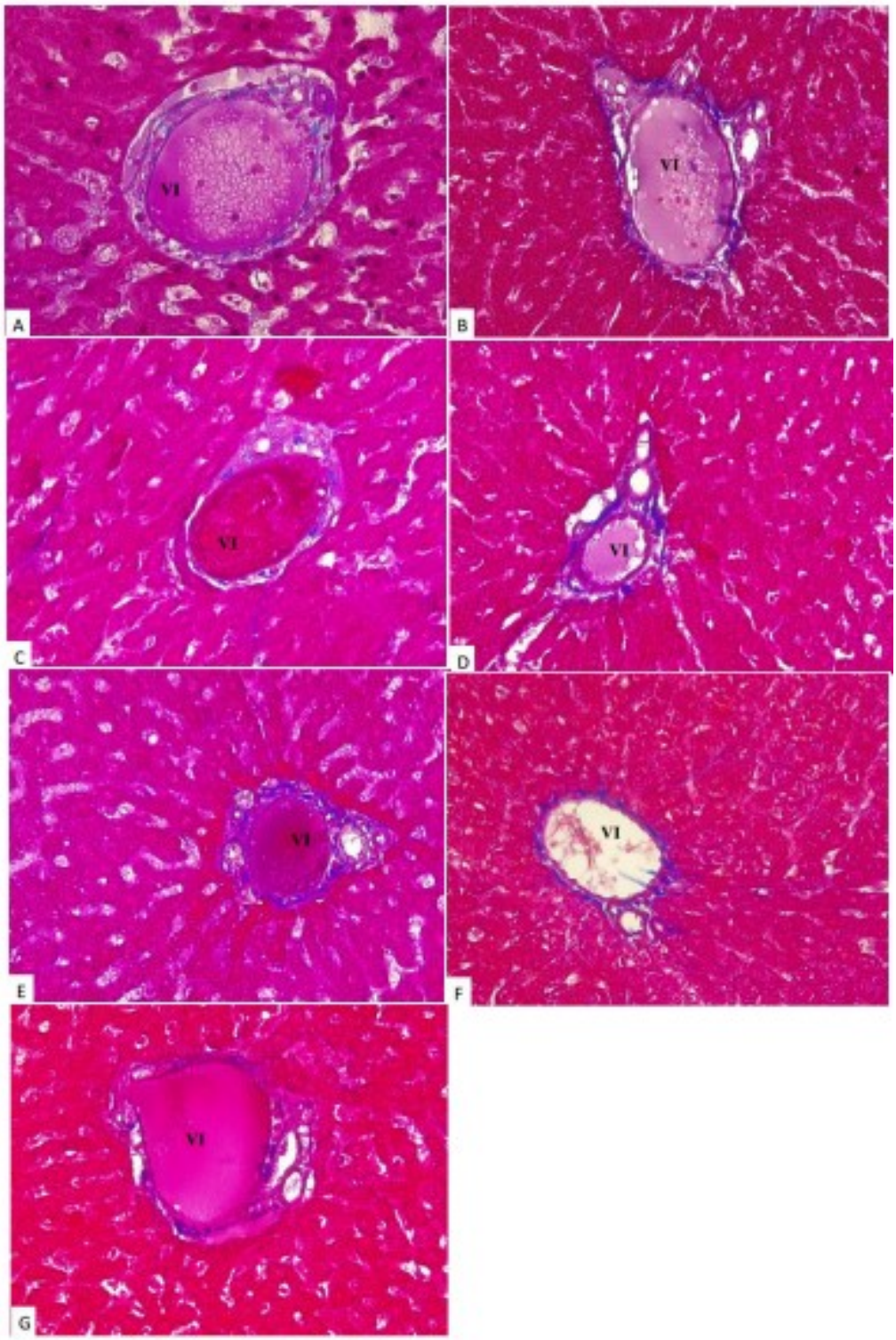

Figure 3. Histological structure of liver group A) control, B) placebo control, C) K3, D) K4, E) K5, F) K6, and G) K7. Showing Portal veins (VP) structure. MAF stained, 10x40 magnification

ACKNOWLEDGEMENTS

This research was supported by BPPTNBH Faculty of Biology, Universitas Gadjah Mada year 2018. We thank our colleagues who provided insight and expertise that greatly assisted the research; Sodrina Adani, S.Si., M. Fajar Shidik, Rahma Nabila, and Alfisyahr.

REFERENCES

Carlton, W.W. & McGavin, M.D., 1995, *Special Veterinary Pathology*, 2nd ed., Mosby, United States of America.

Chiang, J., 2014, 'Liver Physiology: Metabolism and Detoxification', in L.M. McManus & R.N.. Mitchell (eds), *Pathobiology of Human Disease,* pp. 1770-1782, Elsevier, San Diego.

Bedossa, P., 1994, Intraobserver & Interobserver Variations in Liver Biopsy Interpretation in Patients with Chronic Hepatitis C, *Hepatology* 20(1), 15-20.

BPS, 2002, Statistik Perkebunan, Jakarta.

Harlita, 2016, Potensi Ekstrak Kulit Biji Mete (*Anacardium occidentale* L.) Sebagai Agen Penurun Kapasitas Reproduksi Tikus Putih (*Rattus norvegicus* Berkenhout 1769) betina [Potential of Cashew Seed Extract (*Anacardium occidentale L.*) As a Reducing Reproductive Capacity of White Rats (*Rattus norvegicus* Berkenhout 1769) female], *Doctoral thesis*, pp. 2-14, Universitas Gadjah Mada, Yogyakarta.

Herlina, 2013, Potensi Biotoksikan Ekstrak Etanolik Kulit Biji Mete (*Anacardium occidentale* L.) Pada Sistem Reproduksi Jantan Tikus Putih (*Rattus norvegicus* Berkenhout 1769) Galur Wistar [Biotoxic Potential of Ethanolic Extract of Cashew Seed Skin (*Anacardium occidentale L.*) in Male Reproduction System of White Rat (*Rattus norvegicus* Berkenhout 1769) Wistar Strain] *Master thesis,* pp. 122-132, Universitas Gadjah Mada, Yogyakarta.

Hou, L., Kai, L., Yuhong, L., Shuang, M., Xunming, J. & Lei, L., 2016, Necrotic Pyknosis is a Morphologically and Biochemically Distinct Event from Apoptotic Pyknosis, *Journal of Cell Science* 129, 3084-3090.

King, N.W. & Joseph, A., 1996, 'Intracellular and Extracellular Deposition; Degenerations', in T.C. Jones, R.D. Hunt & N.W. King (eds.) *Veterinary Pathology* 6th ed., Blackwell Publishing Professional, USA.

Patel, S., 2016, Emerging Adjuvant Therapy for Cancer; Propolis and Its Constituents, *J Diet Suppl.* 13:245-268

Sativani I., 2010, Pengaruh Pemberian Deksametason Dosis Bertingkat Per Oral 30 Hari Terhadap Kerusakan Sel Hepar Tikus Wistar [The Effect of Giving Dexamethasone 30-Day Oral Dose to Wistar Rat Cell Damage], *Undergraduate thesis,* Universitas Diponegoro, Semarang.

Journal of Tropical Biodiversity and Biotechnology
Volume 04, Issue 03(2019): 119 — 123
DOI: 10.22146/jtbb.42306

Research Article

Kidney Function Test of Female Wistar Rat (*Rattus norvegicus* Berkenhout, 1769) of Subchronic Toxicity Test of *Arthrospira maxima* and *Chlorella vulgaris*

Mulyati[1]*, Anita Yuliana[1], Slamet Widiyanto[1]
1) Faculty of Biology, Universitas Gadjah Mada, Jl. Teknika Selatan, Sekip Utara, Yogyakarta, 55128

Corresponding author, telp.: 08122766569, email address : mulyati.biougm@ugm.ac.id

Keywords:
A. maxima
C. vulgaris
creatinine
urea
kidney index
glomerular structure

Article history:
Submitted 31/12/2018
Revised 11/11/2019
Accepted 22/11/2019

ABSTRACT

Arthrospira maxima and *Chlorella vulgaris* are contained a high protein and antioxidant levels that can be used as functional foods or supplements to improve health. Furthermore, this material needs to be monitored for safety. The aims of this research were determined the subchronic toxicity test of microalgae *A. maxima* and *C. vulgaris* on kidney function. Parameters of this research were creatinine levels, urea levels, kidney index, and histological structure of the kidney glomerular. Besides that, the progression of body weight was observed. Five teen female Wistar rats (*Rattus norvegicus* Berkenhout,1769) divided into three groups randomly were one control group and two treatment groups using *A. maxima* and *C. vulgaris* in the same dose were 2500 mg/kg of body weight. Subchronic toxicity test was conducted by oral gavage every day during 90 days — the measurement of creatinine levels and urea levels on the 30th, 60th, and 90th day. Kidney index and glomerular histology of rat's kidney was prepared after necropsy at the end of this research. Base on the results, it can be concluded that consume of *Arthrospira maxima,* and *Chlorella vulgaris* at 2500 mg/kg of body weight increased creatinine and urea levels. Bodyweight, kidney index, and pathological glomerular cells of histological kidney were still in normal value.

INTRODUCTION

Microalgae are micro-sized algae groups. It has many types, which are commonly found in marine and freshwater with sizes ranging from a few micrometers to several hundred micrometers. Microalgae are a source of nutrition that provides several bioactive compounds, polymers, peptides, fatty acids, carotenoids, sterols, and toxins (Kim, 2015).

Microalgae have been investigated as a food or nutrition source for humans and animals for more than six decades (Liu et al., 2014). Two species of microalgae that can be used as functional foods and are the focus of this study are *Arthrospira maxima* and *Chlorella vulgaris*. Over the past 2-3 decades, millions of people around the world have consumed *A. maxima* as a food supplement. *A. maxima is* also rich in vitamin B12, carotene, omega-3 and omega-6 as essential fatty acids and antioxidants, which are very beneficial for the health of the body (Affan et al., 2015). *Chlorella vulgaris* also has high protein content, rich in vitamins, minerals, omega-3 fatty acids, and carotenoids (Gouveia et al., 1995).

In the body of *A. maxima* and *C. vulgaris* will be digested, absorbed, and distributed through the blood circulation. Afterwards, follow the metabolic process in the liver and then the soluble elements in the water will be excreted through the kidneys. Therefore, it is necessary to monitor the safety of *A. maxima* and *C. vulgaris* as functional foods through subchronic oral toxicity studies. The effects of microalgae *A. maxima* and *C. vulgaris* on kidney function was evaluated. Bodyweight, kidney index, creatinine level, urea level, and glomerular structure were chosen to evaluate the kidney function.

MATERIALS AND METHODS

Materials

This research was conducted from October 2017 to March 2018. Orally sub-chronic toxicity test and measuring of creatinine and urea level was conducted at the Integrated Laboratory Research and Testing (*Laboratorium Penelitian dan Pengujian Terpadu, LPPT*) UGM. Preparation of kidney using paraffin method was done at the Laboratory of Animal Structure and Development of the Faculty of Biology UGM. This experiment was done after obtaining approval from the Animal Ethics Commission Team with certificate number 00096/04/LPPT/VII/2017. The material used in this research was *Arthrospira maxima,* and *Chlorella vulgaris* powder was obtained from *Blue Green Alga* (BGA) *Biotechnology*, female Wistar rat (Rattus norvegicus Berkenhout 1769) 2 months. The chemicals needed in the process of histology preparations are distilled water, NBF (Neutral Buffered Formalin), alcohol, toluol, enthelan, paraffin, paraffin I, II, and III, xylol, Meyer`s albumin, Erlich Hematoxylin, and Eosin-Y 1-2%.

Methods

Subchronic orally toxicity test

Before done the treatment, rats acclimated for five days. Giving feed and drinking Reverse Osmosis water *ad libitum*. Fifteen rats divided into three groups and treated microalgae of 2500 mg/kg of body weight in dose, five rats treated with *A. maxima*, five rats treated with *C. vulgaris*, and five rats for control with force-fed distilled water as much as 2 mL.

Blood Chemistry Analysis

The blood sample was collected through the orbital sinus after anesthetist with ketamine on the day of 30 (D-30), 60 (D-60), and 90 (D-90) respectively. The creatinine and urea level was measured with the colorimetric method using a spectrophotometer, conducted at *LPPT* UGM.

Preparation of Glomerular Kidney Histology

The kidney organ was fixed in Neutral Buffered Formalin (NBF) solution for 48 hours. Washing with 70% alcohol, then dehydration using graded alcohol from a concentration of 70%, 80%, 90%, 96%, and absolute respectively. The clearing was carried out using toluol overnight. Paraffin infiltration was done in the oven at 60□C. Embedding part of kidney tissue to form paraffin blocks. After that, was done trimming on the paraffin blocks and sectioning with a thickness of 5 µm. Furthermore, the affixing of these coups (+ kidney tissue) was carried out on objects glass and then staining with Hematoxylin-Eosin (HE). Object glass with kidney histological was labelled, observed, and analyzed. The disturbing of cells function or pathological cells state be assessed by determining and calculating of each cell state for all the cells in histological glomerular.

Data of body weight, kidney index, urea level, and creatinine level for evaluating kidney function test tabulated in Microsoft Excel 2016 *software*. The data were statistically analyzed using *one-way ANOVA* with a 95% confidence level. If there is a difference, then followed by *Duncan's Multiple Range Test (DMRT)* using a software program *(software)* SPSS 23. Glomerular structure and pathological cells state were observed descriptively.

RESULTS AND DISCUSSION

Body Weight

In this study, weighing the bodyweight of the animals model was done once a week to observe the effect of the administration of *A. maxima* and *C. vulgaris* on animals model body weight. Data body weight development of female *Wistar* rats for 90 days be shown in Figure 1 and Table 1.

Table 1. Progression of body weight from female Wistar rats (*Rattus norvegicus*, Berkenhout1769) with A. maxima and C. vulgaris treatment in subchronic orally toxicity test

Group	Rats obtained weight (grams)
Control	77.26 ± 21.42 [a]
Arthrospira maxima	77.58 ± 8.72 [a]
Chlorella vulgaris	78.06 ± 10.92 [a]

Based on Figure 1, it can be seen that both control group rats and oral treatment of microalgae *A. maxima* and *C. vulgaris* 2500 mg/kg of body weight for 90 days were obtained the increasing of the body weight. The increasing of the body weight, from the highest to the lowest were treated by *C. vulgaris* > *A. maxima* > control, respectively. The progression of body weight during the treatment (after and before treatment) was presented in Table 1.

In Table 1, it is known that there was no significant difference in the increase of body weight between each group of rats. This increase in body weight is due to the increasing age and the growing of that animal experiment. This is also supported by feeding and drinking *ad libitum*.

Kidney Index

Kidney index was calculated at the end of this

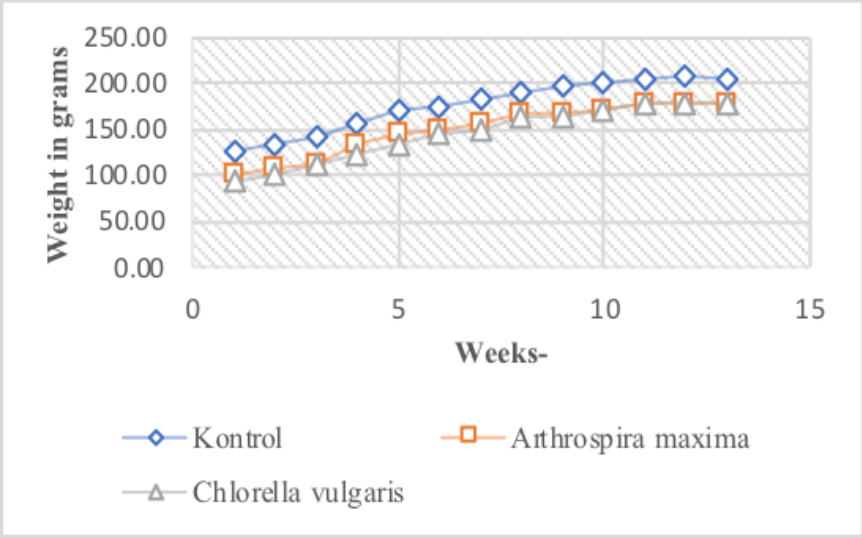

Figure 1. Bodyweight of female Wistar rats (*Rattus norvegicus*, Berkenhout 1769) with *A. maxima* and *C. vulgaris* treatment in a subchronic oral toxicity test

research from the kidney weight and body weight. Kidney index is one of the kinds of organ index that is to observe the condition of the organs in the body. Kidney index of this research is displayed in Table 2 underneath.

Based on Table 2, the results of statistical tests on kidney index of all groups were not significantly different. Due to it can be seen that there is no change in kidney organ mass. This result showed that the rat was given microalgae *A. maxima* and *C. vulgaris* not giving adverse effect on the kidney index so that the kidney can be function normally.

Table 2. Kidney Index of female rats (*Rattus norvegicus*, Berkenhout 1769) Wistar strain with *A. maxima* and *C. vulgaris* treatment in subchronic orally toxicity test

Group	Kidney Index
Control	0.9970 ± 0.07 [a]
Arthrospira maxima	0.9968 ± 0.07 [a]
Chlorella vulgaris	0.9969 ± 0.10 [a]

Creatinine Level

Creatinine level in blood was indicated of kidney function in the body. Creatinine is nitrogen waste products from the catabolism of creatine phosphate and muscle activity (contraction and relaxation), so increasing of creatinine level significantly in the blood is indicate there is a disorder of renal function or increasing activity of skeletal muscle. Normally, the value of rats creatinine levels according to Giknis and Clifford (2008) is 0.2-0.6 mg/dL. Increasing creatinine levels in control, treated *A. maxima,* and *C. vulgaris* on 90th days is still in the normal range according to previous research (Giknis and Clifford, 2008). This result has shown that no impairment of kidney functions in creatinine excretion from the body. Table 3 were presented the result of this research.

According to the Table 3 on the 30th day, the creatinine levels of the control group rats showed significant differences with the two treatment groups, this was because the weight in normal rat was higher than the two treatments. According to Perrone et al. (1992), the other factors that influence creatinine level in the blood is muscle mass. If seen in the control group, it is reviewed based on time on the 30th, 60th and 90th days there is not significantly different. Whereas in the treatment groups the administration of *A. maxima* and *C. vulgaris,* there were significant differences on the 60th and 90th day. This is due to the increase in muscle mass and weight due to the growth of the rat treated groups. The increase in creatinine levels in the treated rat can also be due to other functions of these two microalgae as antidepressant substances so that stress due to stress treatment can be reduced and does not disturb with body activity. So that increased body activity raises muscle activity which also increases creatinine levels as well. On days 30th, 60th, and 90th creatinine levels between groups did not significantly different. So *A. maxima* and *C. vulgaris* dose 2500 mg/kg could increase the creatinine levels but does not cause toxic effects because the value does not exceed the reference range of normal creatinine levels in the rat.

Urea Level

In blood, urea level was measured to assess the kidney function of the body. Urea is the excrete from the catabolism of the amino acid as end-product of protein catabolism. So, the level of Urea in the blood can be used to diagnosis for support of kidney function.

Table 3. Creatinine levels of female Wistar rats (*Rattus norvegicus*, Berkenhout 1769) with *A. maxima* and *C.vulgaris* treatment in subchronic orally toxicity test

Group	Creatinine levels in mg/dL		
	H-30	H-60	H-90
Control	0.42 ± 0.03^{bx}	0.46 ± 0.03^{ax}	0.50 ± 0.05^{ax}
Arthrospira maxima	0.36 ± 0.05^{ax}	0.43 ± 0.07^{axy}	0.51 ± 0.07^{ay}
Chlorella vulgaris	0.33 ± 0.06^{ax}	0.47 ± 0.04^{ay}	0.45 ± 0.11^{ay}

Noted in value a,b,c were compared among in the column x,y noted were compared value among in line

Ureum levels of the group that given *C. vulgaris* are increased from the 30th to the 90th day. While the control and treatment of *A. maxima* increased on the 60th day and decreased on the 90th day. The Urea level from this research was presented in Table 4.

According to Table 4. can be seen on the 30th day after the administration of treatment there was a significant difference between the control group and the administration of microalgae groups *A. maxima* and *C. vulgaris*. However, on the 60th and 90th days, there were no significant differences between each group. The high protein content in both microalgae caused an increase in ureum levels in the treatment of microalgae *A. maxima* and *C. vulgaris*. According to Verdiansah (2016), urea is the end product of protein and amino acid catabolism, produced by the liver and distributed through the blood circulation for filtration by kidney especially in the glomerulus. So high protein levels can cause high urea levels. According to Andrade and Costa (2007), *A. maxima* contains up to 50-70 % protein of the dry weight. Similarly, *Chlorella vulgaris* which has a high protein content, total protein in *C. vulgaris* reach 55 - 67% from dry biomass (Safi et al., 2014). However, the following month, the rat was able to adapt well so there is no significant difference in urea levels.

If reviewed based on time differences, there will be no change significant urea levels in all three groups on 0, 30th, 60th, and 90th day. This shows that the consumption of microalgae *A. maxima* and *C. vulgaris* does not cause changes in the urea significant. Thing presumably, protein levels in microalgae *A. maxima* and *C. vulgaris* can be obtained metabolized properly by the body of the test rat. Thus, giving microalgae *A. maxima* and *C. vulgaris* is not toxic to blood urea levels.

Glomerular Kidney Histology

The kidneys are one of the body's vital organs that regulate the metabolic process and excretion of various substances from the body in the form of urine. Glomerular is the part of the kidney that the site of the important process for waste in the blood. This research was focused on the glomerular histological structure which plays an important role in the filtration process. The glomerular structure was shown in Figure 2.

The result of the control group it can be observed that there is a pyknotic cell nucleus of 0.35% and a karyorrhexis cell nucleus of 0.35% in cells found in the glomerulus. In the treatment group *A. maxima* there was observed damage in the form of a pyknotic nucleus of 1.39%, a karyorrhexis nucleus of 0.88%, and vacuolization of 1.41%. In the treatment group, *C. vulgaris* can be observed damage in the form of picnotic nucleus of 1.80%, karyorrhexis cell nucleus of 0.52%, and vacuolization of 1.52%.

Histological observations of the presence of pyknotic, karyorrhexis, and vacuolization in the treatment group were still within normal limits with a low percentage. This can be due to *C. vulgaris* and *A. maxima* which function as antioxidants. *C. vulgaris* as an antioxidant can be used to prevent kidney damage, as in previous studies conducted by Susatyo et al. (2018) that *C. vulgaris* extract can reduce kidney damage exposed to CCl4. The ability of *C. vulgaris* extract provides protection against oxidative stress and free radicals associated with antioxidant compounds in it. Some antioxidants in *C. vulgaris* extract are lutein, a-carotene, b-carotene, ascorbic acid, chlorophyll, and tocopherol. Antioxidants that have the most important role in preventing damage from free radicals are carotene. This compound can remove a single oxygen and peroxide compound through a redox reaction.

A. maxima contain phycocyanin which functions antioxidants to prevent damage caused by free radicals. Phycocyanin is also useful in the *renoprotective*. *A. maxima* also contain beta carotene which also functions as a lipophilic antioxidant. *A. maxima* contain beta carotene around 700-1700 mg/kg. Overdose is unlikely to occur because beta-carotene is not toxic cumulatively and bioavailability have been verified in preclinical and clinical studies. Carotenoids are the second most important pigment group found in algae (Zakaria et al., 2016). Damage due to treatment *A. maxima* and *C. vulgaris* at a dose of 2500 mg/kg of body weight for 90 days has not caused damage to the glomerular structure.

Table 4. Urea level of female rats (*Rattus norvegicus*, Berkenhout 1769) Wistar strain with *A. maxima* and *C. vulgaris* treatment in subchronic orally toxicity test

Groups	Urea levels in mg/dL		
	H-30	H-60	H-90
Control	34.36 ± 2.35^{ax}	42.74 ± 9.70^{ax}	38.92 ± 5.30^{ax}
Arthrospira maxima	40.20 ± 5.97^{abx}	40.60 ± 6.86^{ax}	37.08 ± 4.80^{ax}
Chlorella vulgaris	42.06 ± 6.08^{bx}	42.12 ± 4.75^{ax}	43.68 ± 7.31^{ax}

Noted in value a,b,c were compared among in the column x,y noted were compared value among in line

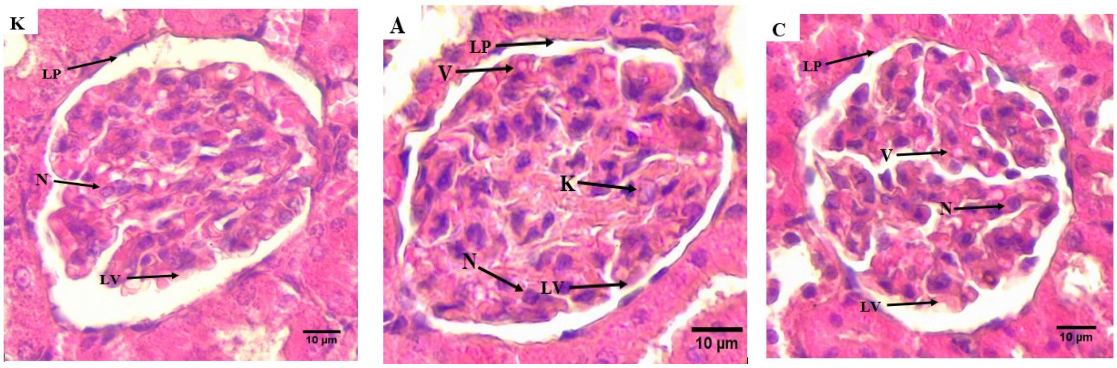

Figure 2. Glomerular microscopic of female rats (Rattus norvegicus, Berkenhout 1769) Wistar Strain with *A. maxima* and *C. vulgaris* treatment in subchronic orally toxicity test. C) Control, A) Treated by *Arthrospira maxima* , C) treated by *C. vulgaris*. Visible parietal lamina (LP), visceral lamina (LV), normal cells (N), karyorrhexis (K) cells, and vacuolization (V).

CONCLUSIONS

Based on the results, it can be concluded that the microalgae subchronic orally toxicity test *Arthrospira maxima* and *Chlorella vulgaris* 2500 mg/kg of body weight in dose increase blood creatinine and urea levels but are still normal value. There were no damage histological structures of the glomerular kidney of female Wistar rats (*Rattus norvegicus* Berkenhout, 1769).

ACKNOWLEDGEMENTS

We would like to thank all those who helped in the completion of this research, our Microalgae group research (Rohmi Salamah, Tika Chandra, Kholidatus Silmi, and Deni Putri).

REFERENCES

Affan, M-A., Lee, D-W., Al-Harbi, S. M., Kim, H-J., Abdulwassi, N.I., Heo, S-J., Oh, C., Park, H-S., Ma, C.W., Lee, H-Y., & Kang, D-H., 2015, Variation of *Spirulina maxima* biomass production in different depths of urea-used culture medium, *Brazilian Journal of Microbiology* 46(4), 991-1000.

Gouveia, L., Veloso, V., Reis, A., Fernandes, H., Novais, J. & Empis, J, 1995, Evolution of pigment composition in Chlorella vulgaris, *Bioresource Technology* 57(2), 157- 163.

Kim, S-K., 2015, *Handbook of Marine Microalgae: Biotechnology Advances,* pp. 1-33, Elsevier, London.

Liu, J., Sun, Z. & Gerken, H., 2014, *Recent Advances in Microalgal Biotechnology,* OMICS Group International, Foster City, CA.

Safi, C., Zebib, B., Merah, O., Pontalier, P-Y. & Vaca-Garcia, C., 2014, Morphology, composition, production, processing, and applications of Chlorella vulgaris, *Renewable and Sustainable Energy Reviews* 35: 265-278.

Susatyo, P., Rifanda, A.A., Simanjuntak, S.B.I. & Chasanah, T., 2018, Antioxidant Effect of *Chlorella vulgaris* on Wistar Rat Kidney Induced by CCl4: A Histopathological Review, *Biosaintifika* 10(1), 169-175.

Verdiansah, 2016, Pemeriksaan Fungsi Ginjal [Renal Function Tests], *Cermin Dunia Kedokteran* 43(2), 148-154.

Elzawahry, Z.A., Abass, M.A., El-Haleem, M.R., Hamid, R.I., & Atteia, H.H., 2016, Spirulina protects against tacrolimus-induced hepatic and renal toxicity in rats: A biochemical and histological study, *Journal of Toxicology and Environmental Health Sciences* 8(7), 47-55.

9 772540 958004

KONSORSIUM BIOTEKNOLOGI INDONESIA
Indonesian Biotechnology Consortium

KOBI